Geoscience Frontiers 9 (2018) 355–375

HOSTED BY

ELSEVIER

Contents lists available at ScienceDirect

China University of Geosciences (Beijing)

Geoscience Frontiers

journal homepage: www.elsevier.com/locate/gsf

Research Paper

Detrital zircon geochronology of the Lützow-Holm Complex, East Antarctica: Implications for Antarctica–Sri Lanka correlation

Yusuke Takamura [a], Toshiaki Tsunogae [a,b,*], M. Santosh [c,d], Yukiyasu Tsutsumi [e]

[a] Graduate School of Life and Environmental Sciences, University of Tsukuba, Ibaraki 305-8572, Japan
[b] Department of Geology, University of Johannesburg, Auckland Park 2006, South Africa
[c] School of Earth Sciences and Resources, China University of Geosciences Beijing, 29 Xueyuan Road, Beijing 100083, China
[d] Centre for Tectonics Resources and Exploration, Department of Earth Sciences, University of Adelaide, SA 5005, Australia
[e] Department of Geology and Paleontology, National Museum of Nature and Science, Ibaraki 305-0005, Japan

ARTICLE INFO

Article history:
Received 1 May 2017
Received in revised form
24 July 2017
Accepted 29 August 2017
Available online 9 September 2017

Keywords:
The northern Lützow-Holm–Vijayan Complex
Zircon U–Pb geochronology
Crustal evolution
Tectonic correlations
Gondwana supercontinent

ABSTRACT

The Lützow-Holm Complex (LHC) of East Antarctica has been regarded as a collage of Neoarchean (ca. 2.5 Ga), Paleoproterozoic (ca. 1.8 Ga), and Neoproterozoic (ca. 1.0 Ga) magmatic arcs which were amalgamated through the latest Neoproterozoic collisional events during the assembly of Gondwana supercontinent. Here, we report new geochronological data on detrital zircons in metasediments associated with the magmatic rocks from the LHC, and compare the age spectra with those in the adjacent terranes for evaluating the tectonic correlation of East Antarctica and Sri Lanka. Cores of detrital zircon grains with high Th/U ratio in eight metasediment samples can be subdivided into two dominant groups: (1) late Meso- to Neoproterozoic (1.1–0.63 Ga) zircons from the northeastern part of the LHC in Prince Olav Coast and northern Sôya Coast areas, and (2) dominantly Neoarchean to Paleoproterozoic (2.8–2.4 Ga) zircons from the southwestern part of the LHC in southern Lützow-Holm Bay area. The ca. 1.0 Ga and ca. 2.5 Ga magmatic suites in the LHC could be proximal provenances of the detrital zircons in the northeastern and southwestern LHC, respectively. Subordinate middle to late Mesoproterozoic (1.3–1.2 Ga) detrital zircons obtained from Akarui Point and Langhovde could have been derived from adjacent Gondwana fragments (e.g., Rayner Complex, Eastern Ghats Belt). Meso- to Neoproterozoic domains such as Vijayan and Wanni Complexes of Sri Lanka, the southern Madurai Block of southern India, and the central-western Madagascar could be alternative distal sources of the late Meso- to Neoproterozoic zircons. Paleo- to Mesoarchean domains in India, Africa, and Antarctica might also be distal sources for the minor ~2.8 Ga detrital zircons from Skallevikshalsen. The detrital zircons from the Highland Complex of Sri Lanka show similar Neoarchean to Paleoproterozoic (ca. 2.5 Ga) and Neoproterozoic (ca. 1.0 Ga) ages, which are comparable with those of the LHC, suggesting that the two complexes might have formed under similar tectonic regimes. We consider that the Highland Complex and metasedimentary unit of the LHC formed a unified latest Neoproterozoic suture zone with a large block of northern LH–Vijayan Complex caught up as remnant of the ca. 1.0 Ga magmatic arc.

1. Introduction

Previous petrological, geochemical and geochronological studies on East Africa–India–Sri Lanka–East Antarctica region, which corresponds to the central part of the East African–Antarctic Orogen, suggest that the region was formed through a sequence of complex subduction–accretion–collision processes of various arc and continental components during the latest Neoproterozoic to Cambrian Gondwana amalgamation (e.g., Meert, 2003; Jacobs and Thomas, 2004; Collins and Pisarevsky, 2005; Collins et al., 2007a,b, 2014; Meert and Lieberman, 2008; Santosh et al., 2009, 2014, 2015, 2016, 2017, and reference therein). The Lützow-Holm Complex (LHC) of East Antarctica has been regarded as one of the examples of Neoproterozoic to Cambrian high-grade metamorphic terranes

* Corresponding author. Graduate School of Life and Environmental Sciences, University of Tsukuba, Ibaraki 305-8572, Japan.
E-mail address: tsunogae@geol.tsukuba.ac.jp (T. Tsunogae).
Peer-review under responsibility of China University of Geosciences (Beijing).

http://dx.doi.org/10.1016/j.gsf.2017.08.006

formed during this orogenic event (e.g., Hiroi et al., 1991; Shiraishi et al., 1994). Recent geochemical and geochronological studies proposed that the LHC is composed of at least three Neoarchean (ca. 2.5 Ga), Paleoproterozoic (ca. 1.8 Ga), and Neoproterozoic (ca. 1.0 Ga) magmatic arcs and was formed by collision of these terranes (e.g., Dunkley et al., 2014; Takahashi et al., 2017). The LHC has been correlated with other Gondwana fragments, particularly the Sri Lankan basement which is composed of two Neoproterozoic magmatic arcs (Wanni and Vijayan Complexes) and a suture zone (Highland Complex) between them. Yoshida et al. (1992) proposed that the sedimentary units of the LHC along the Lützow-Holm Bay (LHB) region (Ongul and Skallen Groups) could be correlated to those of the Highland Complex based on structural patterns and lithological similarities. Shiraishi et al. (1994) also regarded the LHC as a supracrustal basin developed in a suture zone with the Highland Complex during the final phase of Gondwana assembly. Kazami et al. (2016) discussed geochemical and geochronological similarities of meta-igneous rocks from the LHC and the Kadugannawa Complex of Sri Lanka. Similar metamorphic *P–T* conditions from the two regions are also discussed (e.g., Yoshida et al., 1992; Takamura et al., 2015; Osanai et al., 2016a,b). In contrast, there are also some major differences between the two regions, particularly with regard to geochronology. For example, the LHC contains remnants of Neoarchean (ca. 2.5 Ga) magmatic arcs (e.g., Shiraishi et al., 1994, 2008; Dunkley et al., 2014; Tsunogae et al., 2014, 2016), which have not been reported from Sri Lanka. In this study, we will therefore compare geological, petrological, and geochronological features of the LHC and Sri Lanka and evaluate the correlation of the two regions for further unraveling the tectonic evolution and terrane assembly during Gondwana amalgamation.

Zircon is a common accessory mineral in crustal rocks, and possesses the properties of physical and chemical durability against weathering and metamorphism. Therefore, geochronological investigations of detrital zircon and comparison of their age spectra with those of adjacent terranes are common approaches to understand the evolution of orogens and reconstruction of continental fragments (e.g., Gebauer et al., 1989; Cawood et al., 2003; Tsutsumi et al., 2009; Kuznetsov et al., 2014). The detrital zircon ages from the Highland Complex have been well studied. For example, dominant Paleoarchean to Paleoproterozoic (ca. 3.5–1.7 Ga) detrital zircons have been obtained from the Highland Complex (Kröner et al., 1987; Hölzl et al., 1994; Dharmapriya et al., 2016; Takamura et al., 2016). Recent studies also reported early to middle Neoproterozoic (ca. 1.0–0.7 Ga) ages for detrital zircons from the complex (Sajeev et al., 2010; Dharmapriya et al., 2015, 2016). Kitano et al. (2015a,b) argued the difference of dominant detrital zircon ages between the eastern (ca. 2.0–1.5 Ga) and western (ca. 1.0–0.7 Ga) parts of the Highland Complex. In contrast, only a few report of Neoarchean to Neoproterozoic detrital zircon ages have been presented from the LHC (e.g., Shiraishi et al., 1994, 2003; Dunkley et al., 2014), and they are restricted only from the LHB region. No data are available from the region along Price Olav Coast in the eastern part of the complex. Systematic correlation of age spectra of the LHC with those from other Gondwana fragments has not been done so far.

This study reports new geochronological data on detrital zircon grains in metasediments from eight localities in the LHC, compares their age spectra with available geochronological data from other Gondwana fragments such as Sri Lanka, southern India, and Madagascar, and evaluates their implications on paleogeographic correlations.

2. Geological background

2.1. General geology and metamorphism

The Lützow-Holm Complex is located from southwest to northeast along the Prince Harald and Sôya Coasts of Lützow-Holm Bay, and Prince Olav Coasts of East Antarctica (Fig. 1). It is bordered with the western Rayner Complex to the east, and the Yamato–Belgica Complex and the Sør Rondane Mountains to the west and south, although the boundaries are not exposed. The LHC is dominantly composed of felsic to intermediate orthogneisses (e.g., charnockite, biotite-hornblende gneiss) with various metasedimentary rocks (pelitic and psammitic rocks, quartzite, and marble) and metabasites (mafic to ultramafic granulites and amphibolite) (e.g., Shiraishi et al., 1989). Metamorphic grade of the complex increases from amphibolite-facies in the northeast to granulite-facies in the southwest (e.g., Hiroi et al., 1991) (Fig. 1). The highest-grade metamorphic rocks are exposed at Rundvågshetta in the southernmost part of the complex where peak *P–T* condition is as high as 1040 °C and 13–15 kbar (e.g., Kawasaki et al., 2011). Similar ultrahigh-temperature (UHT) metamorphic conditions have been reported from granulites in adjacent localities, such as Skallen and Skallevikshalsen (Osanai et al., 2004; Yoshimura et al., 2008). In contrast, Tsunogae et al. (2014) estimated peak *P–T* condition for charnockites from Rundvågshetta and adjacent Vesleknausen as 800–850 °C, and suggested that the UHT event is a local and only recorded in dry Mg–Al-rich pelitic rocks in this region. Lower peak metamorphic *P–T* conditions have been estimated for the transition zone between granulite- and amphibolite-facies zones such as 750 °C at 7.2–7.5 kbar for Tenmondai Rock (Hiroi et al., 1983), and 770–790 °C at 7.7–9.8 kbar for Akarui Point (Kawakami et al., 2008). In Akarui Point, however, higher temperatures of 825–900 °C were obtained by the application of ternary-feldspar geothermometry (Nakamura et al., 2013). Iwamura et al. (2013) reported peak UHT metamorphism (900–920 °C at 5–6 kbar) and clockwise *P–T* path from sapphirine- and spinel-bearing metagabbro from Akarui Point, and proposed that the LHC might be separated into several crustal blocks by shear zones as inferred from geophysical data of Nogi et al. (2013).

2.2. Geochronology

Available geochronological data from the LHC suggest late Neoproterozoic to early Cambrian (600–520 Ma) high-grade metamorphism (e.g., Shiraishi et al., 1994, 2003, 2008; Asami et al., 1997; Hokada and Motoyoshi, 2006; Tsunogae et al., 2014, 2015, 2016). Shiraishi et al. (1994) performed systematic SHRIMP zircon U–Pb dating for ortho- and paragneisses from several localities in the LHC (e.g., Austhovde, Rundvågshetta, Telen, Ongul, Akarui Point) and obtained peak metamorphic ages as 550–520 Ma. Asami et al. (1997) reported CHIME ages for monazite in biotite gneiss from East Ongul and Mt. Vechernyaya as 537–533 Ma. Hokada and Motoyoshi (2006) also performed CHIME monazite age dating for pelitic granulites from Skallen and obtained two age groups; 650–580 Ma of prograde metamorphic age and 560–500 Ma of peak metamorphic age. Dunkley (2007) reported a spread of SHRIMP zircon age from ca. 600 to 500 Ma in the LHC, and concluded that the 550–530 Ma event corresponds to retrograde metamorphism of the LHC after the peak metamorphism at >550 Ma. Tsunogae et al. (2014) obtained 591 ± 3 Ma and 548 ± 7 Ma SHRIMP zircon ages from partially molten feldspathic rock from Vesleknausen, and interpreted the ages corresponding to prograde partial-melting stage and retrograde metamorphic stage, respectively, suggesting that the peak

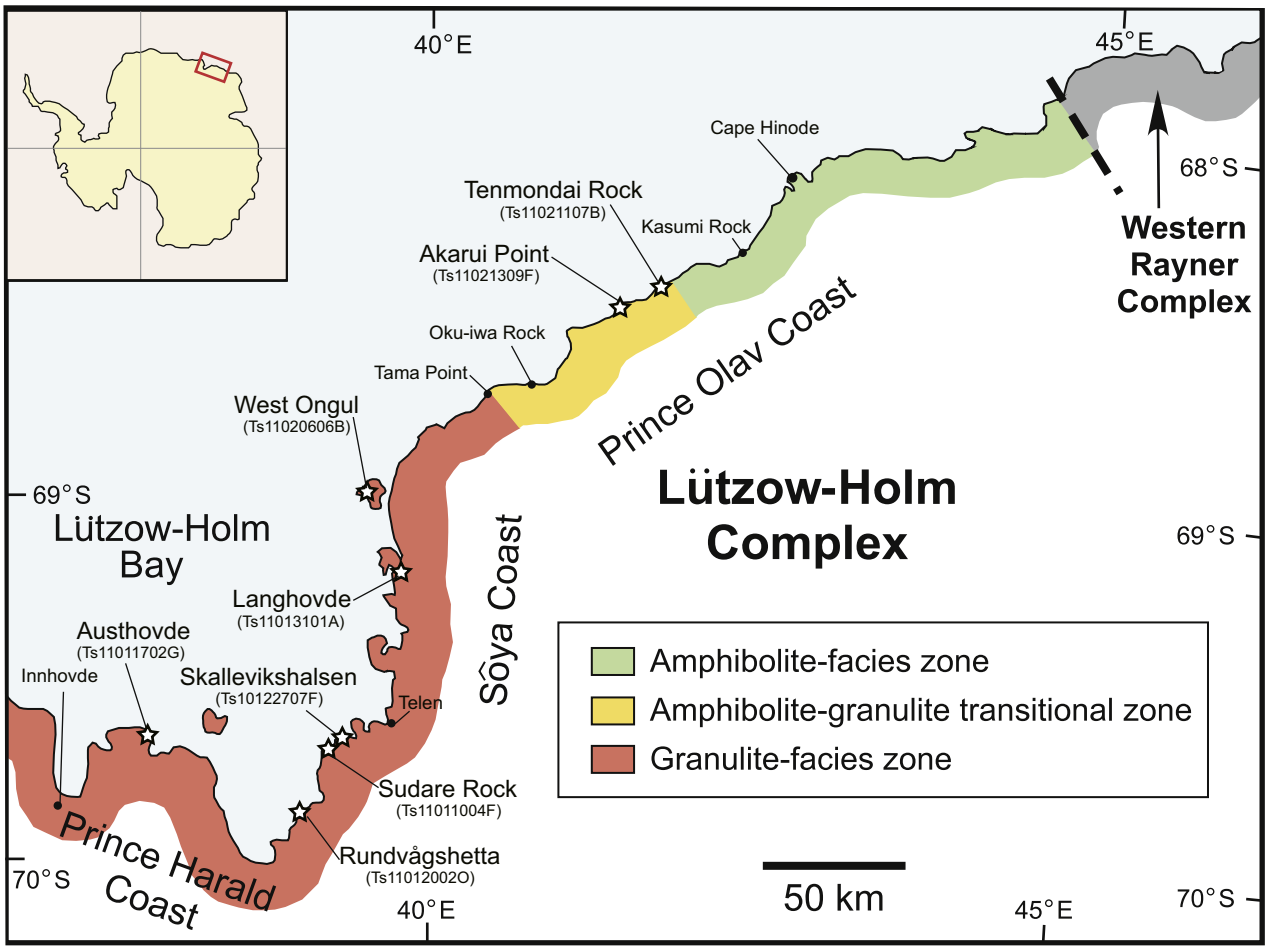

Figure 1. Generalized geological framework of the Lützow-Holm Complex, East Antarctica (after Hiroi et al., 1991), with sample localities shown by star notations.

metamorphism took place between 591 Ma and 548 Ma. Kawakami et al. (2016) identified older (~650–580 Ma) and younger (~560–500 Ma) age populations from both zircon and monazite in pelitic gneiss from Skallevikshalsen and interpreted that the rocks might have experienced polymetamorphism. Fraser et al. (2000) reported K/Ar and $^{40}Ar/^{39}Ar$ ages of hornblende and biotite in granulites from Rundvågshetta, and inferred this region cooled to 350–300 °C by ca. 500 Ma. Rb–Sr mineral isochron age obtained for hornblende-biotite gneiss from Oku-iwa Rock (431 ± 14 Ma) has also been regarded as a cooling age (Kawano et al., 2006).

Protolith magmatic ages have also been reported for meta-igneous rock in the LHC. The Nd-model ages from the north-eastern (Prince Olav Coast and northern Sôya Coast) and western LHC (Prince Harald Coast) show late Meso- to early Neoproterozoic ages of ca. 1.25–1.0 Ga (Shiraishi et al., 2008 and references therein). In contrast, Nd-model ages from the southern LHC (southern Sôya Coast) indicate Neoarchean to early Paleoproterozoic ages (ca. 2.70–2.29 Ga). Shiraishi et al. (2003) reported early Neoproterozoic zircon U–Pb ages from orthogneisses including trondhjemite from Cape Hinode (1040–913 Ma) and hornblende-biotite gneiss from Innhovde (1028, 992 and 924 Ma), and proposed possible arc magmatism during early Neoproterozoic. Tsunogae et al. (2015) also reported early Neoproterozoic zircon U–Pb ages (999–965 Ma) for felsic orthogneisses from Kasumi Rock, Tama Point, Innhovde and Hutatu Iwa as the timing of protolith magmatism. Kazami et al. (2016) obtained slightly younger but nearly consistent magmatic ages (847 Ma) with some older xenocrysts (1026–881 Ma) and ages of subsequent thermal events (807–667 Ma) for felsic orthogneiss from Akarui Point. On the other hand, Shiraishi et al. (1994, 2008) reported Neoarchean (ca. 2.5 Ga) magmatic zircons from Ongul and Rundvågshetta regions. Similar 2.5 Ga magmatic ages were obtained from Vesleknausen, Sudare Rock, and Botnutten (e.g., Dunkley et al., 2014; Tsunogae et al., 2014, 2016), suggested Neoarchean crustal growth. Recent studies reported Paleoproterozoic magmatic zircon ages of ca. 2.1–1.8 Ga for orthogneisses from Austhovde, Skallevikshalsen, Skallen, and Telen (Dunkley et al., 2014; Takahashi et al., 2017).

Detrital zircon ages were also reported from metasediments in the LHC. Shiraishi et al. (1994, 2003) analyzed zircon grains in metasediments and obtained Archean to Paleoproterozoic ages (2887–1855 Ma) from West Ongul, Telen, and Rundvågshetta, and Neoproterozoic (1064–966 Ma) ages from Telen. Dunkley et al. (2014) also reported Archean to Paleoproterozoic (ca. 3.3–1.8 Ga) detrital zircon ages from Botnutten, Rundvågshetta, Skallevikshalsen, Telen, and Skarvsnes, and Meso- to Neoproterozoic (1.3–0.62 Ga) ages from Skarvsnes and East Ongul, although detailed petrological and U–Pb isotopic data are not provided.

3. Description of samples

Eight samples of metasediments were collected by the second author from different localities in the LHC during the 52nd Japanese Antarctic Research Expedition (JARE–52) in 2010–2011. The sample localities are shown in Fig. 1. A brief description of the localities

and their geological features as well as salient petrographic characters of the examined samples are given below from northeast to southwest. Among the eight localities, no detrital zircon age has been obtained from Tenmondai Rock, Akarui Point, Langhovde, Sudare Rock, and Austhovde.

3.1. Tenmondai Rock (Ts11021107B)

Sample Ts11021107B is a garnet–biotite–sillimanite gneiss from Tenmondai Rock (S68°26′ 45″; E41°43′15″) in the transition zone of the LHC in Prince Olav Coast (Fig. 1). The sample shows obvious foliation defined by thin (several millimeters) alternation of garnet–biotite-rich and quartzo-feldspathic layers probably formed by migmatization (Fig. 2a). The rock is composed of quartz (30%–40%), plagioclase (30%–40%), garnet (10%–15%), biotite (10%–15%), muscovite (5%–10%), sillimanite (5%–10%), and accessory apatite, monazite, rutile, zircon, pyrite, and Fe–Ti oxide (Fig. 3a). Xenoblastic and fine- to coarse-grained quartz (0.5–5 mm) shows weak wavy extinction. Plagioclase is xenoblastic, fine to coarse grained (0.3–4 mm), and slightly altered. It often coexists with subidioblastic to xenoblastic garnet which is fine to coarse grained (0.3–3 mm) and contains inclusions of apatite, plagioclase, and quartz. Biotite is xenoblastic and fine to medium grained (0.3–1.5 mm). Muscovite often occurs as medium-grained (1–2 mm) flakes together with plagioclase. Sillimanite is idioblastic to subidioblastic and fine to coarse grained (0.3–3 mm). Idioblastic to subidioblastic and fine-grained (0.5 mm) rutile is often included in quartz or biotite. Zircon is also fine grained (0.1–0.2 mm) and rounded, and often included in quartz (Fig. 3a).

3.2. Akarui Point (Ts11021309F)

Sample Ts11021309F (garnet-bearing quartzite) was collected from Akarui Point (S68°30′15″; E41°24′09″) in the transition zone in Prince Olav Coast (Fig. 1). It is alternating with band of pelitic gneiss (Fig. 2b), and composed of quartz (30%–40%) and garnet (30%–40%) with accessory apatite, biotite, rutile, zircon, and opaque minerals (Fe–Ti oxide with minor pyrite) (Fig. 3b). The quartzite also contains secondary limonite (5%–10%) that often occurs around biotite, garnet, and Fe–Ti oxide. Quartz is xenoblastic and coarse grained (1–5 mm), and shows weak wavy extinction. Idioblastic to subidioblastic garnet is coarse grained (2–3 mm) and contains inclusions of apatite, biotite, limonite, quartz, rutile, and Fe–Ti oxide. Biotite is xenoblastic and fine to medium grained (0.3–1 mm). Rutile is subidioblastic to xenoblastic, medium grained (1 mm), and present as inclusions in garnet. Zircon is fine grained (0.1–0.2 mm) and rounded, and mostly present in quartz (Fig. 3b).

3.3. West Ongul (Ts11020606B)

Sample Ts11020606B is a garnet-bearing pelitic gneiss from West Ongul Island (S69°01′16″; E39°30′25″) in the northern Sôya Coast (Figs. 1 and 2c). The sample consists of quartz (30%–40%), plagioclase (30%–40%), garnet (10%–15%), biotite (5%–10%), and K-feldspar (5%–10%) with accessory apatite, graphite, rutile, and zircon (Fig. 3c). Quartz is xenoblastic, fine to coarse grained (0.5–2 mm), and shows weak wavy extinction. Plagioclase is also xenoblastic and fine to coarse grained (0.5–2 mm). Some plagioclase grains contain small quartz inclusions showing simultaneous extinction. Subidioblastic to xenoblastic garnet is medium to coarse grained (1–2 mm), and contains many fine-grained inclusions of apatite and zircon. Xenoblastic and fine- to medium-grained biotite (0.3–1 mm) often coexists with garnet and/or graphite. K-feldspar is xenoblastic and fine to medium grained (0.5–1 mm). Graphite occurs as elongated flakes (0.2–1 mm), some of which coexist with biotite. Idioblastic to subidioblastic rutile is fine grained (0.1–0.8 mm) and occurs as columnar mineral associated with garnet and/or biotite. Rounded and fine-grained zircon (~0.1 mm) occurs as inclusion in quartz, plagioclase, biotite, and garnet (Fig. 3c).

3.4. Langhovde (Ts11013101A)

Sample Ts11013101A from Langhovde (S69°10′43″; E39°37′30″) in the northern Sôya Coast, is a garnet-bearing pelitic gneiss commonly contains boudins of mafic granulite (Fig. 2d). Foliation is defined by alteration of thin (several millimeters) garnet–biotite-rich and quartzo-feldspathic layers. The sample comprises quartz (30%–40%), plagioclase (30%–40%), garnet (10%–15%), and biotite (5%–10%) with minor apatite, rutile, zircon, and pyrite (Fig. 3d). Xenoblastic and fine- to coarse-grained quartz (0.3–5 mm) shows weak wavy extinction. Plagioclase is also xenoblastic and fine to coarse grained (0.3–3 mm). Garnet is subidioblastic to xenoblastic, fine to medium grained (0.3–1 mm), and contains plagioclase and zircon as inclusions. Subidioblastic and fine- to medium-grained biotite (0.3–1 mm) has inclusions such as plagioclase and rutile. Rutile often occurs adjacent to garnet and/or biotite. Zircon is fine grained (~0.1 mm), rounded, and included in quartz, plagioclase, and biotite (Fig. 3d).

3.5. Skallevikshalsen (Ts10122707F)

Sample Ts10122707F is a quartzite collected from Skallevikshalsen (S69°41′43″; E39°18′30″) in the central part of Sôya Coast. It is mostly composed of quartz (>95%) with accessory biotite, calcite, muscovite, and zircon (Figs. 2e and 3e). The quartzite occurs as thick layer alternating with boudinaged garnet amphibolite (Fig. 2e). Xenoblastic and coarse-grained (2–5 mm) quartz exhibits weak wavy extinction. Biotite is subidioblastic and fine to medium grained (0.2–1 mm). Calcite is xenoblastic and fine grained (0.5–0.8 mm). Very fine-grained (<0.1 mm) muscovite often occurs as aggregates and coexists with biotite and calcite. Zircon in the matrix is subidioblastic or rounded, and fine grained (<0.5 mm) (Fig. 3e).

3.6. Sudare Rock (Ts11011004F)

Sample Ts11011004F from Sudare Rock (S69°43′00″; E39°11′49″), located immediately southwest of Skallevikshalsen, corresponds to well-foliated garnet-bearing pelitic gneiss alternating with quartzite layers (Fig. 2f). The rock comprises garnet (30%–40%), plagioclase (40%–50%), biotite (15%–20%), Fe–Ti oxide (5%–10%), and accessory apatite and zircon (Fig. 3f). Garnet is idioblastic to subidioblastic, coarse grained (1–5 mm), and contains abundant inclusions of plagioclase, quartz, Fe–Ti oxide, apatite, zircon, and biotite. Xenoblastic and fine- to medium-grained (0.3–1 mm) plagioclase occurs in matrix or as inclusions in garnet. Some plagioclase grains show granoblastic texture. Biotite is subidioblastic to xenoblastic and fine to medium grained (0.3–1.5 mm). It often coexists with fine- to medium-grained (0.1–1 mm) Fe–Ti oxide. Quartz is fine grained (0.5 mm) and occurs only in garnet as inclusions. Rounded and fine-grained (0.1–0.2 mm) zircon occurs along grain boundaries of garnet, biotite, and plagioclase, or as inclusions in these minerals (Fig. 3f).

3.7. Rundvågshetta (Ts110120020)

Sample Ts110120020 is a quartzite alternating with garnet–spinel–sillimanite-bearing pelitic gneiss in Rundvågshetta

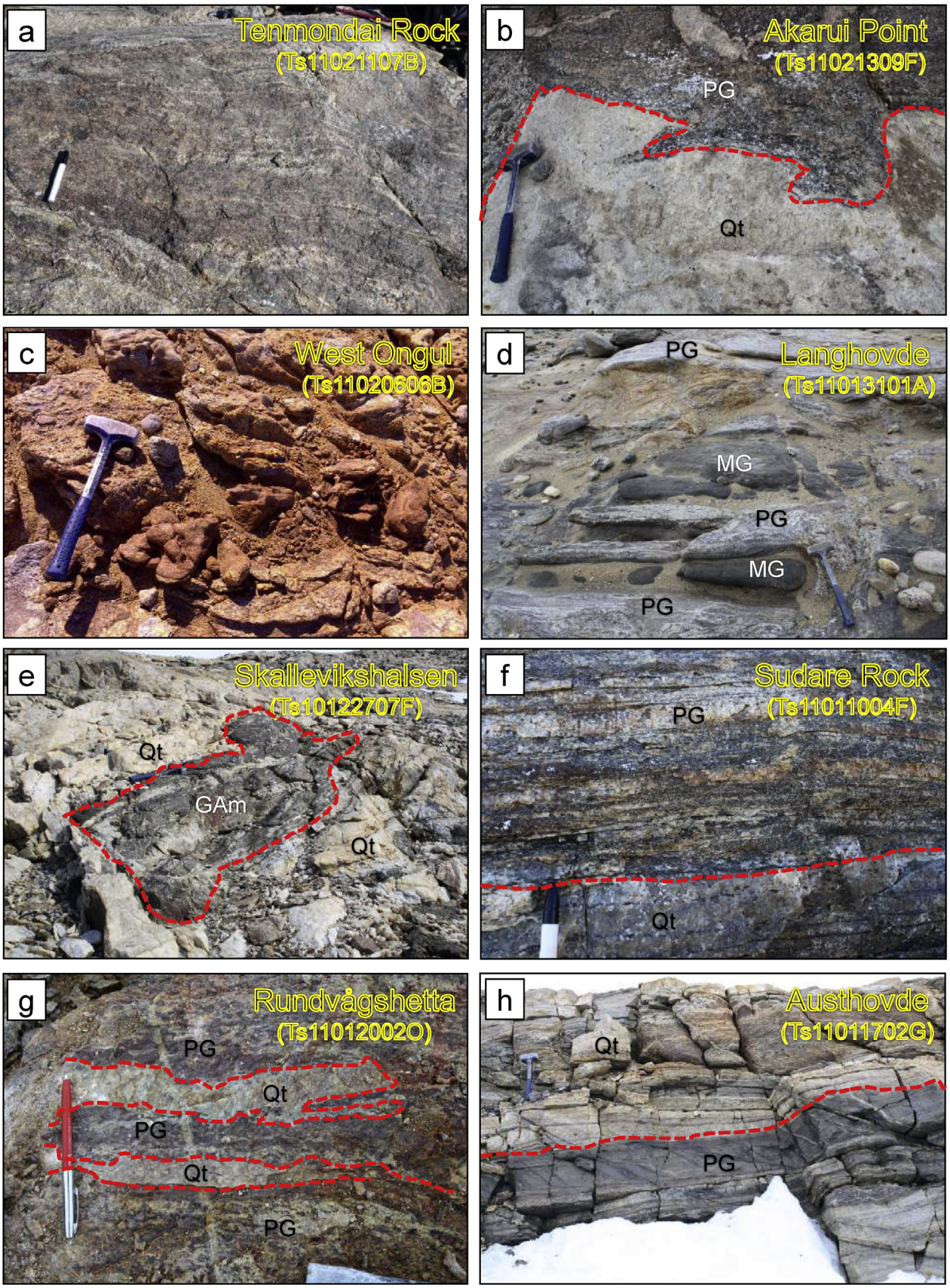

Figure 2. Field photographs of the samples from the Lützow-Holm Complex. (a) Ts11021107B from Tenmondai Rock (pelitic gneiss), (b) Ts11021309F from Akarui Point (quartzite), (c) Ts11020606B from West Ongul (pelitic gneiss), (d) Ts11013101A from Langhovde (pelitic gneiss), (e) Ts10122707F from Skallevikshalsen (quartzite), (f) Ts11011004F from Sudare Rock (pelitic gneiss), (g) Ts11012002O from Rundvågshetta (quartzite), (h) Ts11011702G from Austhovde (quartzite). GAm: garnet amphibolite, MG: mafic granulite, PG: pelitic gneiss, Qt: quartzite.

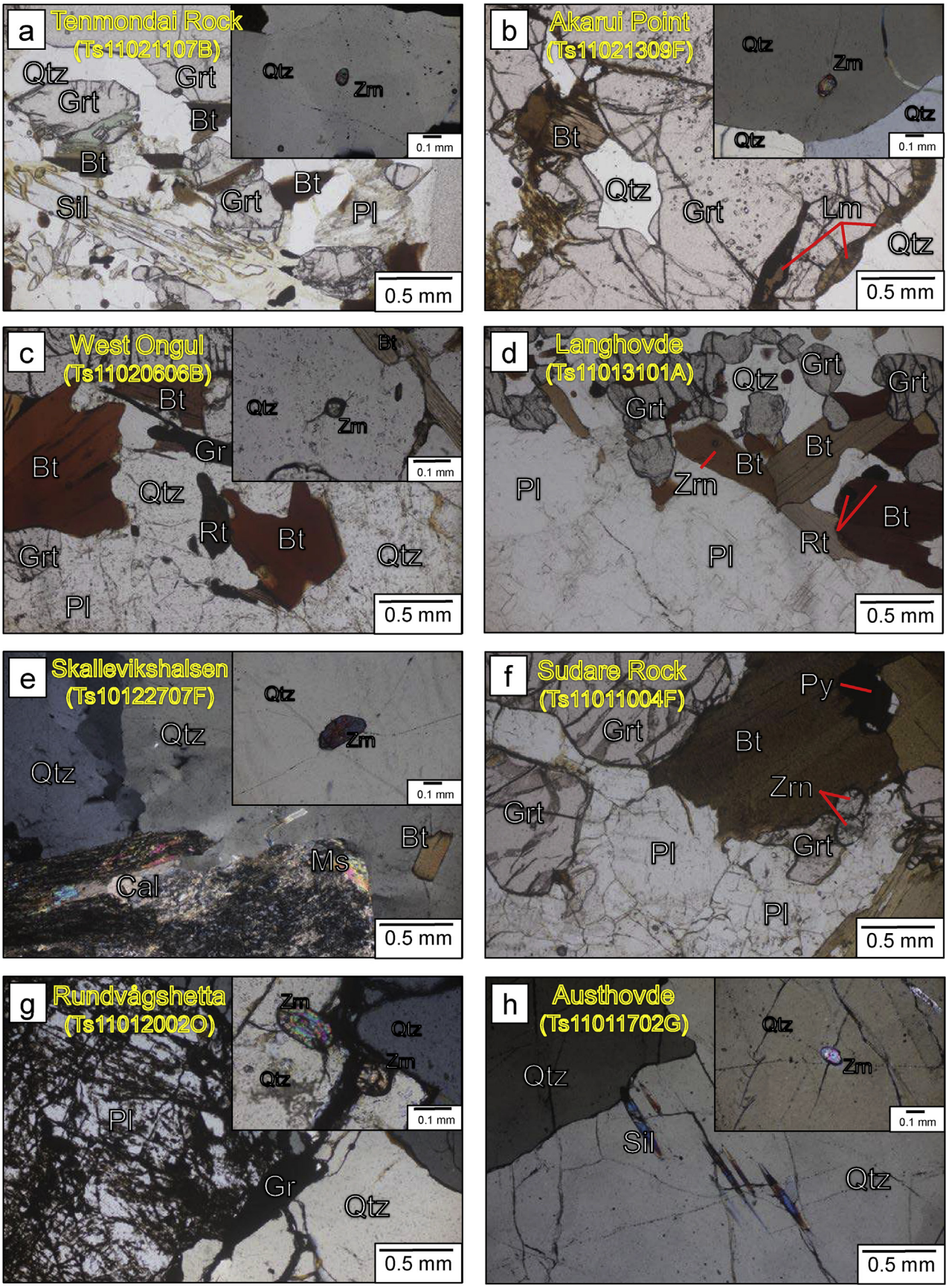

Figure 3. Photomicrographs of thin sections of the samples from the Lützow-Holm Complex, East Antarctica. (a) Ts11021107B, (b) Ts11021309F, (c) Ts11020606B, (d) Ts11013101A, (e) Ts10122707F, (f) Ts11011004F, (g) Ts11012002O, (h) Ts11011702G. Bt: biotite, Cal: calcite, Grt: garnet, Gr: graphite, Lm: limonite, Ms: muscovite Pl: plagioclase, Py: pyrite, Qtz: quartz, Rt: rutile, Sil: sillimanite, Zrn: zircon.

(S69°54′44″; E39°01′28″) from the southern Lützow-Holm Bay area (Fig. 2g). The sample consists of quartz (>90%), plagioclase (5%–10%), and accessory graphite and zircon (Fig. 3g). Quartz is xenoblastic and coarse grained (2–5 mm), and shows weak wavy extinction. Xenoblastic and coarse-grained plagioclase (2–4 mm) is altered along many secondary cracks. Graphite occurs as medium- to coarse-grained flakes (1–3 mm). Zircon is rounded and fine grained (0.2–0.5 mm), and often included in quartz (Fig. 3g).

3.8. Austhovde (Ts11011702G)

Sample Ts11011702G (quartzite) from Austhovde (S69°42′09″; E37°46′10″) in Prince Harald Coast of the western part of Lützow-Holm Bay (Figs. 1 and 2h) is composed of quartz (85%–90%) and minor garnet (5%–10%), plagioclase (5%), and accessory sillimanite, zircon, pyrite, and Fe–Ti oxide (Fig. 3h). Quartz is xenoblastic and coarse grained (>5 mm), and shows weak wavy extinction. Subidioblastic to xenoblastic garnet is medium to coarse grained (1–3 mm) and contains inclusions of quartz, zircon, pyrite, and Fe–Ti oxide. Xenoblastic and fine- to coarse-grained plagioclase (0.3–2 mm) often coexists with garnet, although it is often strongly altered. Accessory sillimanite is fine to medium grained (0.5–1 mm), subidioblastic, and mostly included in quartz. Zircon is rounded and fine grained (0.1–0.2 mm), and occurs in quartz and garnet (Fig. 3h).

4. Analytical method

Zircon U–Pb dating was performed by laser ablation-inductively coupled plasma-mass spectrometry (LA-ICP-MS). Detailed procedures for zircon separation and U–Pb analyses are summarized in Tsutsumi et al. (2012). Zircon grains were separated by heavy liquid (diiodo-methane) and magnetic separation from crushed rock samples, and then purified by hand picking under a binocular microscope. Zircon grains from the studied samples and standard materials were mounted in epoxy resin disc and polished until the surface was flattened with the center of the grains exposed. The FC1 zircon ($^{206}Pb/^{238}U$ = 0.1859; Paces and Miller, 1993) and NIST SRM 610 standard glass were used as standard materials. Backscattered electron and cathodoluminescence (CL) images were obtained using scanning electron microprobe – cathodoluminescence (SEM–CL) equipment, JSM-6610 (JEOL) and a CL detector (SANYU electron), installed at National Museum of Nature and Science, Japan. U–Th–Pb isotopic analyses were carried out using LA-ICP-MS (Agilent 7700x with ESI NWR213 laser ablation system) installed at the National Museum of Nature and Science, Japan. A Nd–YAG laser with a 213 nm wavelength and 5 ns pulse was used for the analysis. A 25-micron spot size and 4–5 J/cm^2 laser power were adopted in this study. He gas was used as the carrier gas instead of Ar gas to enhance a higher transport efficiency of ablated materials (e.g., Eggins et al., 1998). Common Pb corrections for the concordia diagrams and for each age were made using ^{208}Pb (Williams, 1998), on the basis of the model for common Pb compositions proposed by Stacey and Kramers (1975). The upper and lower intercepts in the concordia diagram were calculated using the Isoplot4.15/Ex software (Ludwig, 2008). The degree of discordancy for each analyzed spot was calculated using the method of Song et al. (1996).

5. Results

The results of zircon U–Pb analyses of the metasediment samples are given in Supplementary Table 1. CL images of representative zircons are shown in Fig. 4 together with analyzed spots and U–Pb ages. Concordia diagrams, probability density diagrams with histograms of ages, and Th/U versus age diagrams are shown in Fig. 5. In the following text and figures, ages older or younger than 1.3 Ga are discussed based on $^{207}Pb/^{206}Pb$ or $^{206}Pb/^{238}U$ ages, respectively. The error levels are 1σ.

5.1. Tenmondai Rock (Ts11021107B)

Zircon grains from sample Ts11021107B are translucent and colorless, and show subidioblastic and rounded in habit. The grains show a size range of 50–200 μm and aspect ratios of 2:1 to 1:1 (Fig. 4a). In CL images, most of them show oscillatory-zoned (grain 50), sector-zoned, irregular concentric-zoned, or structureless cores (grains 16 and 45) surrounded by homogeneous and thin rims (grain 14). Some grains also have homogeneous and CL-dark mantle (Fig. 4a). Totally 110 spots were analyzed from 90 zircon grains. Most of the spots are discordant, with 35 spots showing <10% discordance (Fig. 5a). The ages with <10% discordance vary from 2018 ± 17 Ma ($^{207}Pb/^{206}Pb$ age) to 528 ± 6 Ma ($^{206}Pb/^{238}U$ age) (Fig. 5b). Their Th and U contents and Th/U ratio display ranges of 11–5506 ppm, 94–3813 ppm, and 0.01–2.7, respectively (Fig. 5c). Most of the concordant ages of cores are distributed from late Mesoproterozoic to early Neoproterozoic (1141 ± 15 Ma, $^{207}Pb/^{206}Pb$ age to 701 ± 8 Ma, $^{206}Pb/^{238}U$ age) with minor Paleoproterozoic and Mesoproterozoic grains (2018 ± 17 Ma, 1627 ± 27 Ma and 1468 ± 80 Ma, $^{206}Pb/^{238}U$ age), whereas $^{206}Pb/^{238}U$ ages of rims, mantles and some cores with <10% discordance vary from 608 ± 6 Ma to 528 ± 6 Ma (Fig. 5a, b). Th/U ratios of older late Mesoproterozoic to early Neoproterozoic spots show a range of 0.01–0.9 and most of them are higher than 0.1, suggesting their magmatic origin. The Th/U ratios of nine late-Neoproterozoic spots are lower than 0.1 (Fig. 5c) probably suggesting their metamorphic origin. The ratios of other spots are scattered from 0.01 to 2.7.

5.2. Akarui Point (Ts11021309F)

Zircon grains from sample Ts11021309F are translucent, colorless or light brown, and partly rounded. They are subhedral and show ellipsoidal to elongate features with a size range of 50–300 μm and aspect ratios of 3:1 to 1.5:1. Most of the grains have oscillatory-zoned (grains 20 and 50) or irregular concentric-zoned cores surrounded by homogeneous and CL-dark rims in CL images (grains 39 and 50). Some grains show CL-dark homogeneous textures (grain 2) (Fig. 4b). Among 100 analyzed spots on 96 zircon grains, 48 spots show <10% discordance and their ages vary from 1212 ± 17 Ma to 510 ± 5 Ma ($^{206}Pb/^{238}U$ age) (Fig. 5d, e). Th and U contents and Th/U ratio of the spots show ranges of 16–532 ppm, 208–1690 ppm, and 0.01–0.8, respectively (Fig. 5f). Most of cores show late Mesoproterozoic to Neoproterozoic ages (1212 ± 17 Ma to 631 ± 12 Ma, $^{206}Pb/^{238}U$ age), whereas the concordant ages of rims and some cores are distributed from 607 ± 7 Ma to 510 ± 5 Ma (Fig. 5d, e). Th/U ratios of older cores are scattered from 0.1 to 0.8, and most of them are higher than 0.3 (Fig. 5f), suggesting their magmatic origin. In contrast, late Neoproterozoic zircons show lower Th/U ratios of 0.01–0.1, suggesting metamorphic overgrowth.

5.3. West Ongul (Ts11020606B)

Zircon grains from sample Ts11020606B are translucent and colorless. They display spherical to elongate features and their size range and aspect ratios are 50–150 μm in lengths and 2:1 to 1:1, respectively. In CL images, most of the grains exhibit core-rim or core–mantle–rim textures. Core of the grains are oscillatory-zoned (grain 70), concentric-zoned (grain 44), or structureless (grain 64)

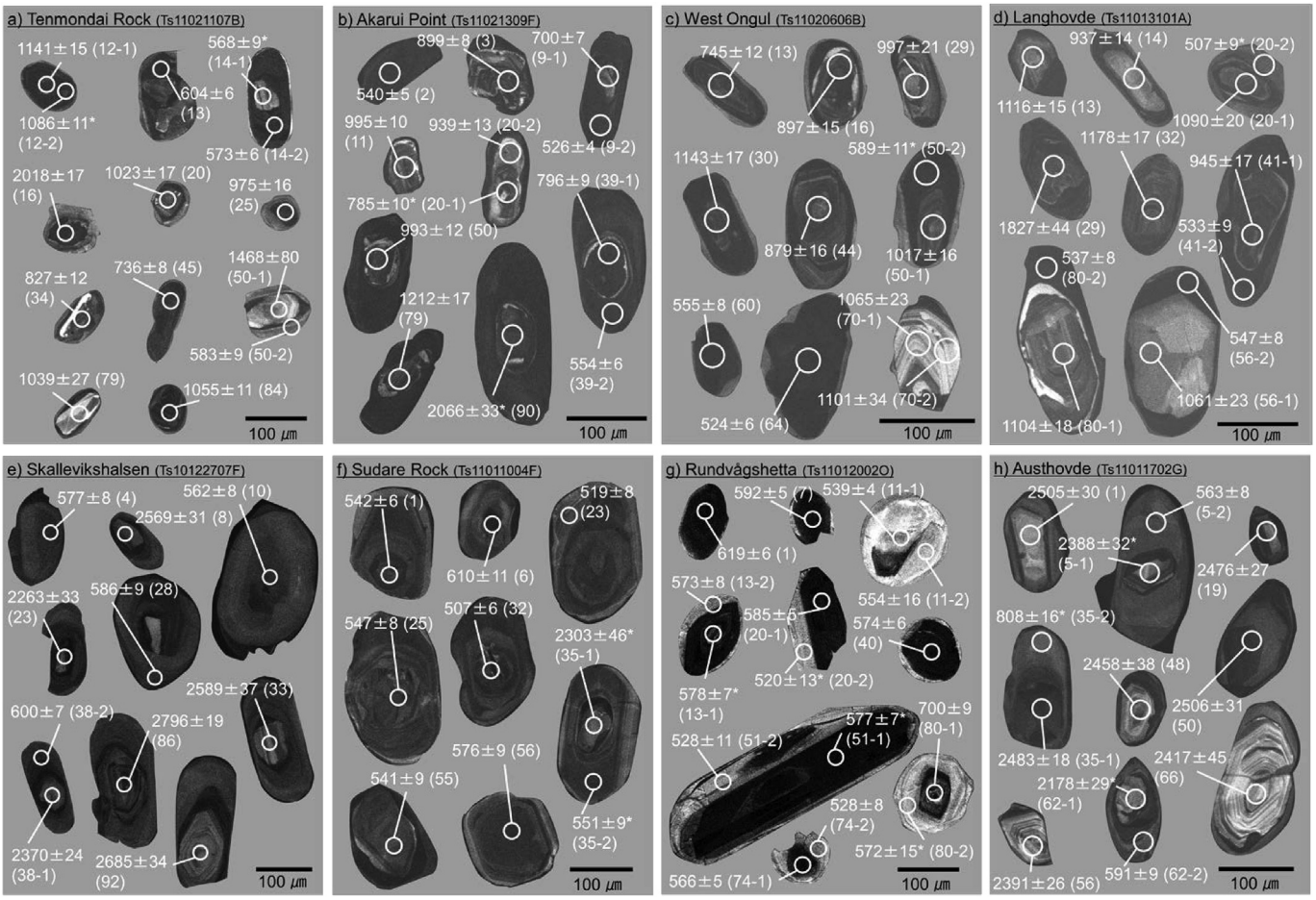

Figure 4. Cathodoluminescence (CL) images of zircon grains from metasediment samples from the Lützow-Holm Complex, East Antarctica. Circles show the spots of U–Pb analysis with age value in Ma and spot number (parentheses). Ages older than 1.3 Ga are shown in $^{207}Pb/^{206}Pb$ age, whereas ages younger than 1.3 Ga are shown in $^{206}Pb/^{238}U$ age. Ages with asterisk indicate discordant (>10% discordance) data. (a) Ts11021107B, (b) Ts11021309F, (c) Ts11020606B, (d) Ts11013101A, (e) Ts10122707F, (f) Ts11011004F, (g) Ts110120020, (h) Ts11011702G.

(Fig. 4c). Most of them are surrounded by homogeneous and CL-dark mantles with homogeneous, thin, and CL-bright rims (Fig. 4c). 81 spots were analyzed from 71 grains with 39 spots showing <10% discordance (Fig. 5g). The results show that the spot ages with <10% discordance vary from 1199 ± 14 Ma to 524 ± 6 Ma ($^{206}Pb/^{238}U$ age) (Fig. 5h). Th and U contents and Th/U ratio of the spots are 10–897 ppm, 38–2701 ppm, and 0.01–1.2, respectively (Fig. 5i). Most of the cores and a few homogeneous grains show late Mesoproterozoic to Neoproterozoic ages as 1199 ± 14 Ma to 697 ± 9 Ma ($^{206}Pb/^{238}U$ age) (Fig. 5h) with the highest peak at ca. 1.0 Ga. Their Th/U ratios show a range of 0.2–1.2, suggesting their magmatic origin. Only three spots on structureless cores display late Neoproterozoic ages (618 ± 12 Ma, 555 ± 8 Ma, and 524 ± 6 Ma, $^{206}Pb/^{238}U$ age) with low Th/U ratios of 0.08–0.01, suggesting their metamorphic origin (Fig. 5i).

5.4. Langhovde (Ts11013101A)

Zircon grains from sample Ts11013101A are translucent, colorless, subhedral, and show ellipsoidal to elongate features with a size range of 50–300 μm in length and aspect ratios of 3:1 to 1.5:1. CL images show that most of the zircon grains have oscillatory-zoned (grain 80), concentric-zoned (grain 20), sector-zoned (grain 56), or structureless cores (grain 14) with homogeneous rims and/or homogeneous and CL-dark mantles (Fig. 4d). Totally 88 spots on 80 grains were analyzed, and the ages of 54 spots with <10% discordance vary from 1827 ± 44 Ma ($^{207}Pb/^{206}Pb$ age) to 521 ± 6 Ma ($^{206}Pb/^{238}U$ age) (Fig. 5j, k). Their Th and U contents and Th/U ratio show ranges of 8–439 ppm, 67–1553 ppm, and 0.01–1.2, respectively (Fig. 5l). Most of the core ages vary from late Mesoproterozoic to middle Neoproterozoic ages (1283 ± 17 Ma to 839 ± 19 Ma, $^{206}Pb/^{238}U$ age) with the highest peak at ca. 1.0 Ga (Fig. 5j, k). One Paleoproterozoic grain with $^{207}Pb/^{206}Pb$ age of 1827 ± 44 Ma was also identified. In contrast, CL-dark rims, mantles, and a few structureless cores exhibit late Neoproterozoic ages as 579 ± 17 Ma to 521 ± 16 Ma. Th/U ratios of late Mesoproterozoic to middle Neoproterozoic spots scatter from 0.06 to 1.2 and most of them are higher than 0.1, whereas Th/U ratios of late Neoproterozoic grains are lower than 0.06 (Fig. 5l). These values clearly suggest that the grains with late Mesoproterozoic to middle Neoproterozoic cores are detrital magmatic zircons, whereas late Neoproterozoic spots are metamorphic zircons.

5.5. Skallevikshalsen (Ts10122707F)

Zircon grains from sample Ts10122707F are translucent and colorless, and show ellipsoidal to elongate features with a size range of 50–300 μm in lengths and aspect ratios of 3:1 to 1.5:1. In CL images, oscillatory-zoned (grain 92), concentric-zoned (grain 86), and structureless cores (grain 10) are present in most zircon

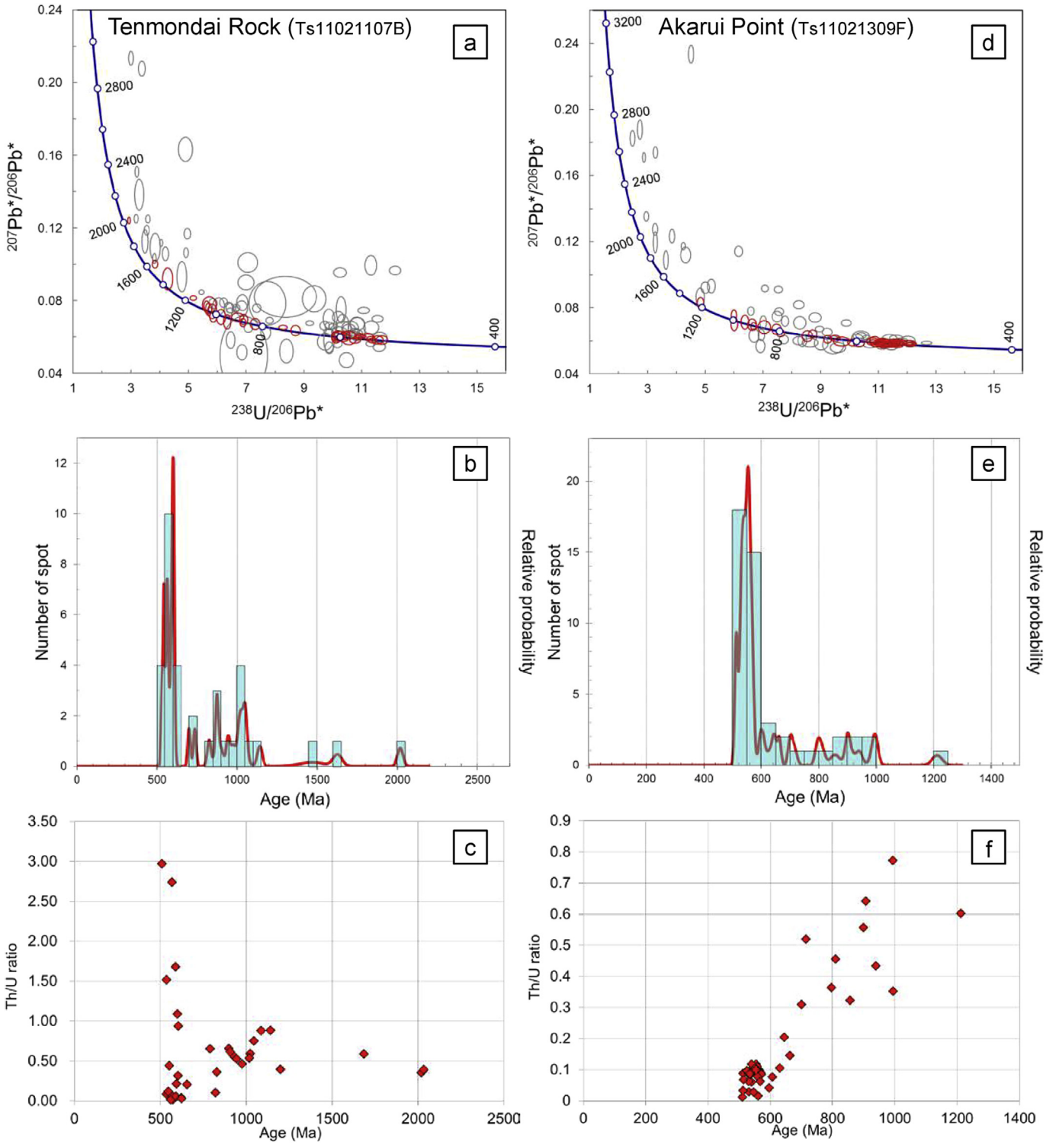

Figure 5. Tera-Wasserburg concordia diagrams (a, d, g, j, m, p, s, v), histograms with probability density plots (b, e, h, k, n, q, t, w), and Th/U versus age diagrams (c, f, i, l, o, r, u, x) of the samples from the Lützow-Holm Complex, East Antarctica. Red and gray circles in concordia diagrams imply concordant (<10% discordance) and discordant (>10% discordance) data, respectively. Histograms show only concordant data. Inset figures exhibit Th/U ratio versus age in Ma. (a–c) Ts11021107B, (d–f) Ts11021309F, (g–i) Ts11020606B, (j–l) Ts11013101A, (m–o) Ts10122707F, (p–r) Ts11011004F, (s–u) Ts11012002O, (v–x) Ts11011702G.

grains, and they are often surrounded by homogeneous rims (Fig. 4e). Some grains have thin and CL-dark rims (Fig. 4e). Totally 96 spots were analyzed from 92 grains. Most of them are discordant, and 33 spots show <10% discordance (Fig. 5m). The ages with <10% discordance vary from 2796 ± 19 Ma ($^{207}Pb/^{206}Pb$ age) to 545 ± 6 Ma ($^{206}Pb/^{238}U$ age) (Fig. 5n). Th and U contents and Th/U ratio of these spots are 25–490 ppm, 49–1211 ppm, and 0.03–1.3, respectively (Fig. 5o). The ages of oscillatory-zoned, concentric-

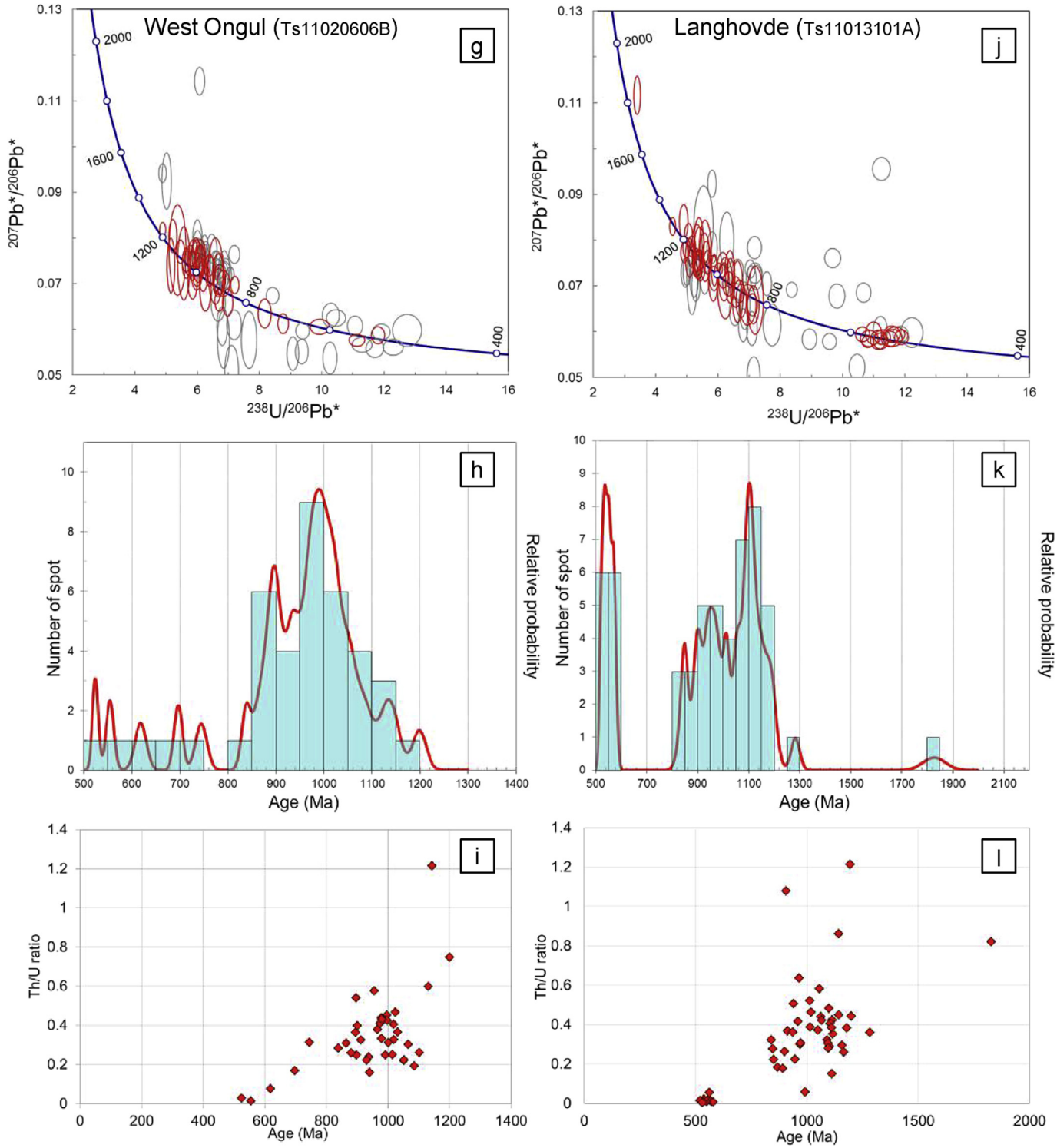

Figure 5. (*continued*).

zoned, and some structureless cores range from Neoarchean to Paleoproterozoic (2796 ± 19 Ma to 1971 ± 92 Ma, $^{207}Pb/^{206}Pb$ age) and most of them show Neoarchean to Paleoproterozoic ages (ca. 2.8–2.4 Ga) (Fig. 5m, n). On the other hand, many homogeneous cores and CL-dark rims exhibit late Neoproterozoic ages (606 ± 7 Ma to 545 ± 6 Ma, $^{206}Pb/^{238}U$ age) (Fig. 4e). Th/U ratios of older grains display a range of 0.3–1.3, suggesting their magmatic origin, whereas late Neoproterozoic grains were probably formed or overprinted during high-grade metamorphism because of their lower Th/U ratios (0.03–0.25) (Fig. 5o).

5.6. Sudare Rock (Ts11011004F)

Zircon grains from sample Ts11011004F are translucent, colorless or light brown, and subhedral. The grains exhibit spherical to elongate features and their size range and aspect ratios are

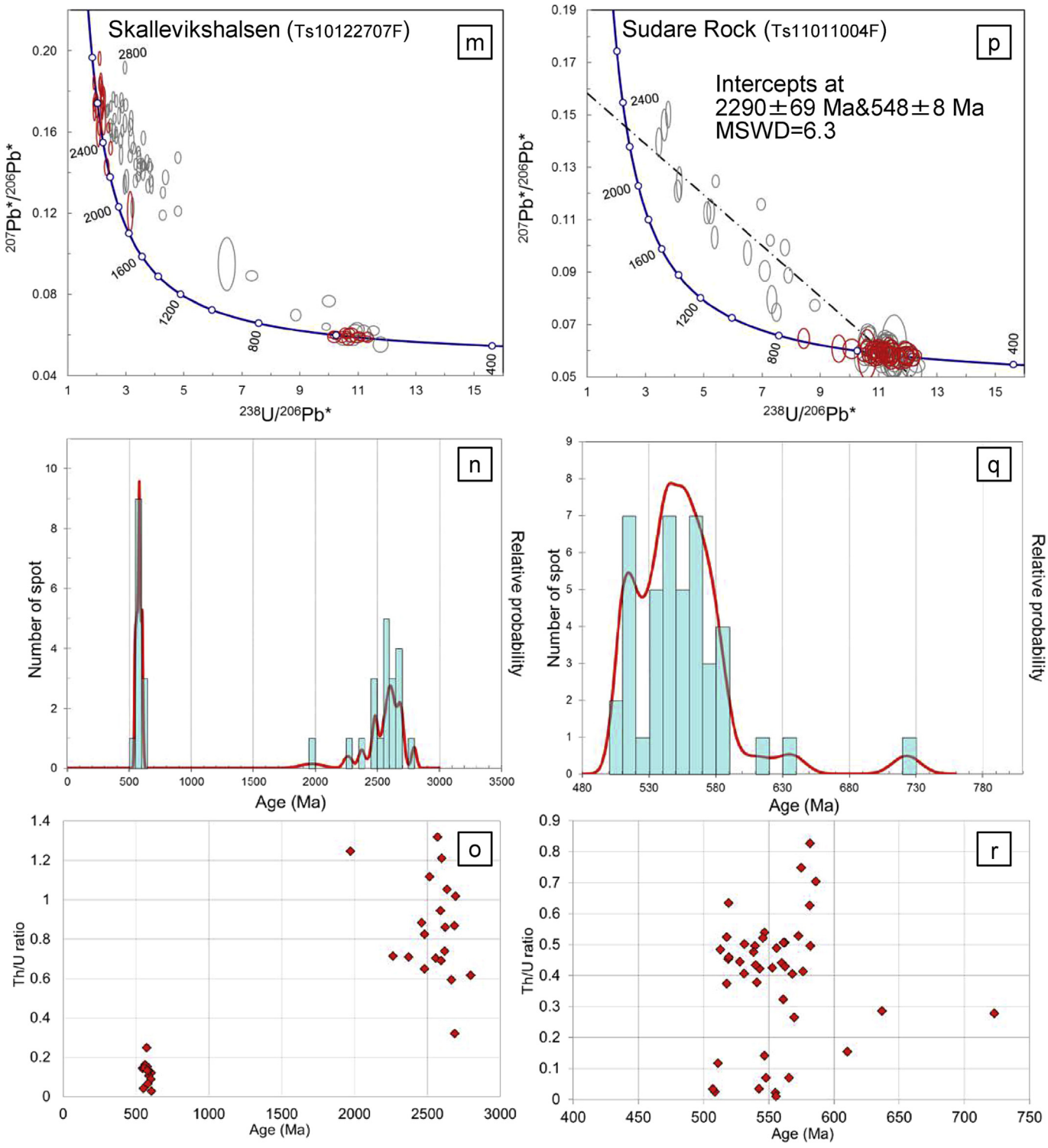

Figure 5. (*continued*).

50–350 μm and 3:1 to 1:1, respectively. Most of the grains have concentric-zoned (grains 1 and 25) and structureless cores (grain 56) surrounded by homogeneous rims (grain 35) in CL images (Fig. 4f). A few grains show oscillatory-zoned cores. Totally 98 spots on 86 grains were analyzed with 44 spots showing <10% discordance (Fig. 5p). These spots with <10% discordance show $^{206}Pb/^{238}U$ ages varying from 723 ± 10 Ma to 507 ± 6 Ma (Fig. 5q). Most of them display late Neoproterozoic age (586 ± 8 Ma to 507 ± 6 Ma), and only three grains are older than 600 Ma (723 ± 10 Ma, 637 ± 10 Ma, and 610 ± 11 Ma) (Fig. 5q). The oldest grain with <10% discordance (723 ± 10 Ma) shows oscillatory-zoning. Th and U contents and Th/U ratio of the grains with <10%

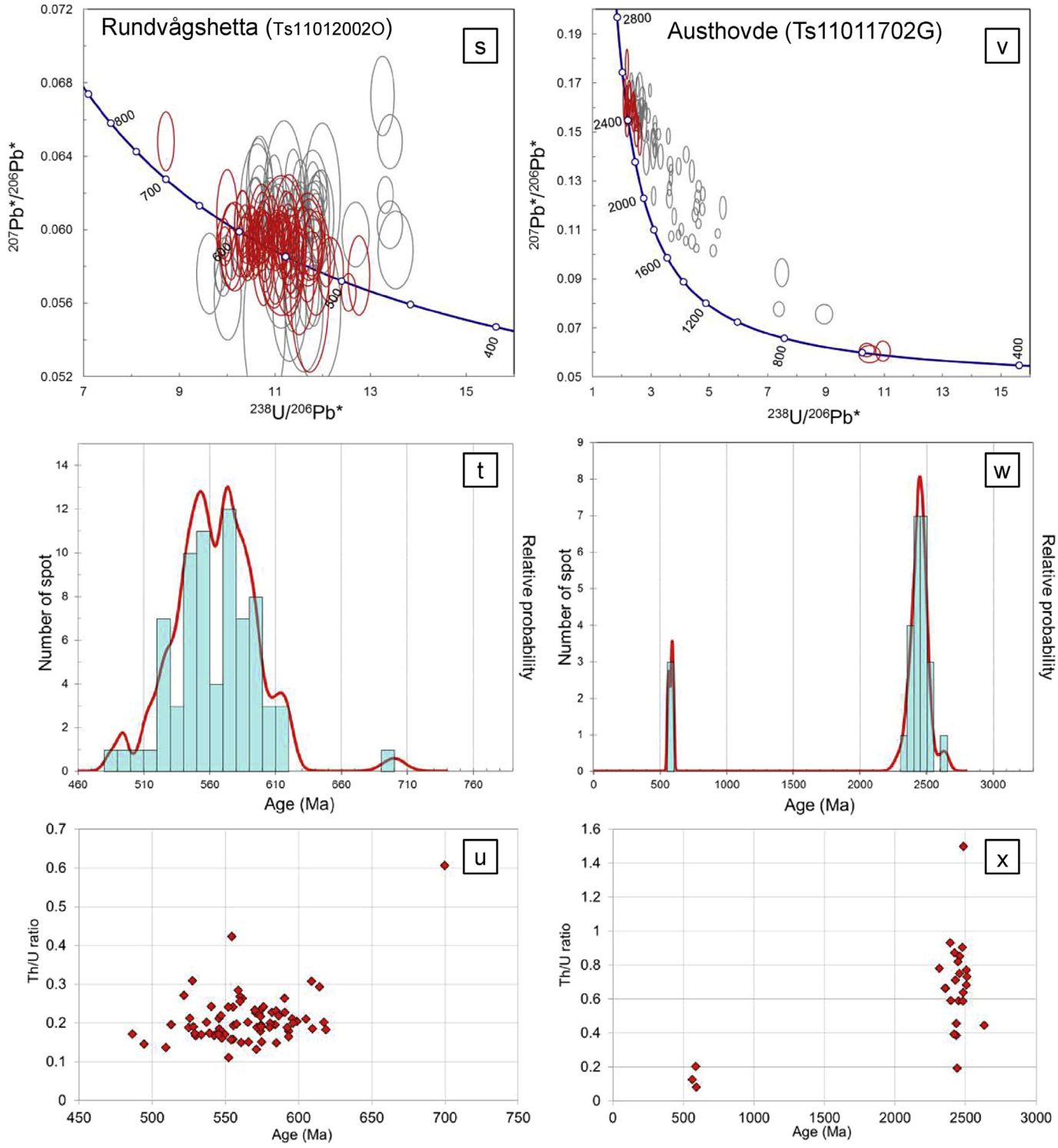

Figure 5. (*continued*).

discordance show ranges of 9–397 ppm, 122–1032 ppm, and 0.01–0.8, respectively (Fig. 5r). Analyzed spots with >10% discordance apparently lie along a discordia with upper and lower intercept ages of 2290 ± 69 Ma and 548 ± 8 Ma, respectively, and MSWD = 6.3 (Fig. 5p). The results indicate that predominant Neoarchean to Paleoproterozoic detrital zircons were partly overprinted during late Neoproterozoic high-grade metamorphism.

5.7. Rundvågshetta (Ts11012002O)

Zircon grains from sample Ts11012002O are translucent, colorless, and light brown. They are subhedral and show spherical to elongate features with a size range of 50–400 μm and aspect ratios of 4:1 to 1:1. CL images show that most of the grains have concentric-zoned (grain 13) or CL-dark structureless cores (grains 1

and 7) with homogeneous and CL-bright rims (grain 80) (Fig. 4g). Among 125 analyzed from 92 grains, 73 spots display low discordance (<10%) and their ages vary from 700 ± 9 Ma to 486 ± 5 Ma ($^{206}Pb/^{238}U$ age) (Fig. 5s, t). Their Th and U contents and Th/U ratio are 58–967 ppm, 140–3484 ppm, and 0.1–0.6, respectively (Fig. 5u). Although most of the cores and rims show late Neoproterozoic ages (619 ± 6 Ma to 486 ± 5 Ma) with low Th/U ratios (0.1–0.4), one core with the highest Th/U ratio of 0.6 shows middle Neoproterozoic age (700 ± 9 Ma) (Fig. 5u), suggesting significant effect of zircon overprinting or overgrowth during late Neoproterozoic high-grade metamorphism.

5.8. Austhovde (Ts11011702G)

Zircon grains from sample Ts11011702G are translucent, colorless, and light brown. The grains show spherical to elongate features with a size range of 50–200 μm and aspect ratios of 3:1 to 1:1. In CL images, most of them have core-rim or core–mantle–rim texture. The cores are oscillatory-zoned (grains 56 and 66), concentric-zoned (grain 48), or structureless (grain 35) surrounded by homogeneous rims and/or mantles (Fig. 4h). Totally 84 spots on 71 grains were analyzed with 26 spots showing <10% discordance (Fig. 5v, w). The spots with <10% discordance vary in age from 2632 ± 37 Ma ($^{207}Pb/^{206}Pb$ age) to 563 ± 8 Ma ($^{206}Pb/^{238}U$ age) (Fig. 5w). Their Th and U contents and Th/U ratio are 23–309 ppm, 73–516 ppm, and 0.08–1.5, respectively (Fig. 5x). The core ages range from Neoarchean to early Paleoproterozoic (2632 ± 37 Ma to 2313 ± 50 Ma) (Fig. 5w). On the other hand, three spots (one rim and two mantles) show late Neoproterozoic ages (591 ± 9 Ma, 587 ± 13 Ma and 563 ± 8 Ma) (Fig. 5v, w). Th/U ratios of Neoarchean to early Paleoproterozoic cores scatter from 0.2 to 1.5, whereas those of late Neoproterozoic spots are lower, 0.08–0.2 (Fig. 5x). These results suggest the Neoarchean to early Paleoproterozoic cores are detrital magmatic grains, whereas the Neoproterozoic zircons are overgrown during metamorphism.

6. Discussion

6.1. Geochronology of detrital zircons of the LHC

Detrital cores of zircons in metasedimentary rocks from eight localities in the LHC exhibit late Mesoproterozoic to Neoproterozoic (1.1–0.65 Ga) and Neoarchean to Paleoproterozoic (2.8–2.4 Ga) ages with dominant peaks of ca. 1.0 Ga and 2.5 Ga (Fig. 6). The late Mesoproterozoic to Neoproterozoic ages were obtained from Tenmondai Rock (ca. 1.1–0.7 Ga; Fig. 5a, b), Akarui Point (ca. 1.2–0.6 Ga; Fig. 5d, e), West Ongul (ca. 1.2–0.7 Ga; Fig. 5g, h), and Langhovde (ca. 1.2–0.8 Ga; Fig. 5j, k) in Prince Olav and northern Sôya Coasts in the northeastern part of the complex, whereas the Neoarchean to Paleoproterozoic ages were obtained from Skallevikshalsen (ca. 2.8–2.4 Ga; Fig. 5m, n) and Austhovde (ca. 2.6–2.4 Ga; Fig. 5v, x) in the southwestern and western parts of the complex. Although detrital cores from Sudare Rock and Rundvågshetta only exhibit predominant late Neoproterozoic ages possibly suggesting intense metamorphic overprint (Fig. 5p, q, s, t), the zircon U–Pb data from Sudare Rock are aligned along a discordia with the upper-intercept age of ca. 2.3 Ga, suggesting the presence of Paleoproterozoic detrital zircons (Fig. 5p).

The new detrital zircon ages reported in this study are comparable with the results of previous studies. For example, Neoproterozoic (844 Ma) detrital zircon age from Akarui Point in the northeastern part of the LHC (Shiraishi et al., 2003) is within the range of our results from Tenmondai Rock and Akarui Point (ca. 1.2–0.6 Ga). Dunkley et al. (2014) reported similar Neoproterozoic (1.1–0.62 Ga) detrital zircon ages from East Ongul in the northern Sôya Coast, which are consistent with our 1.2–0.7 Ga zircons from West Ongul. In contrast, Shiraishi et al. (1994) obtained Archean to Paleoproterozoic (ca. 2.7–1.8 Ga) ages from West Ongul, suggesting that detrital zircons of Ongul region are probably mainly Neoproterozoic with minor population of Neoarchean grains. Predominant late Meso- to Neoproterozoic detrital zircons from Skarvsnes (ca. 1.3–1.0 Ga; Dunkley et al., 2014) are consistent with

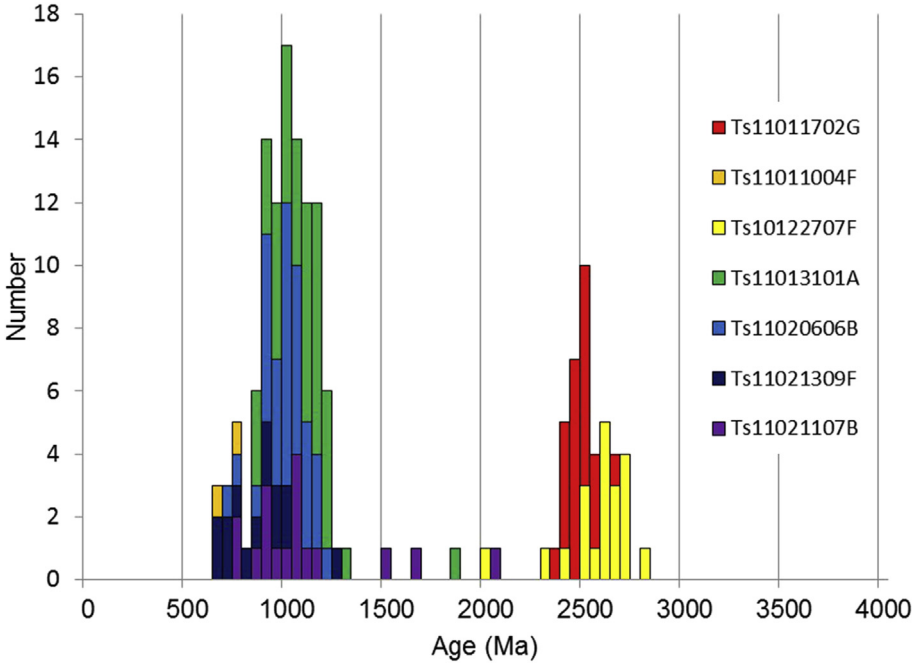

Figure 6. Age data histograms from detrital zircons in the Lützow-Holm Complex, East Antarctica, obtained in this study. Ages older than 1.3 Ga are shown in $^{207}Pb/^{206}Pb$ age, whereas ages younger than 1.3 Ga are shown in $^{206}Pb/^{238}U$ age. Data from sample Ts11012002O are not shown because of the absence of detrital zircon age.

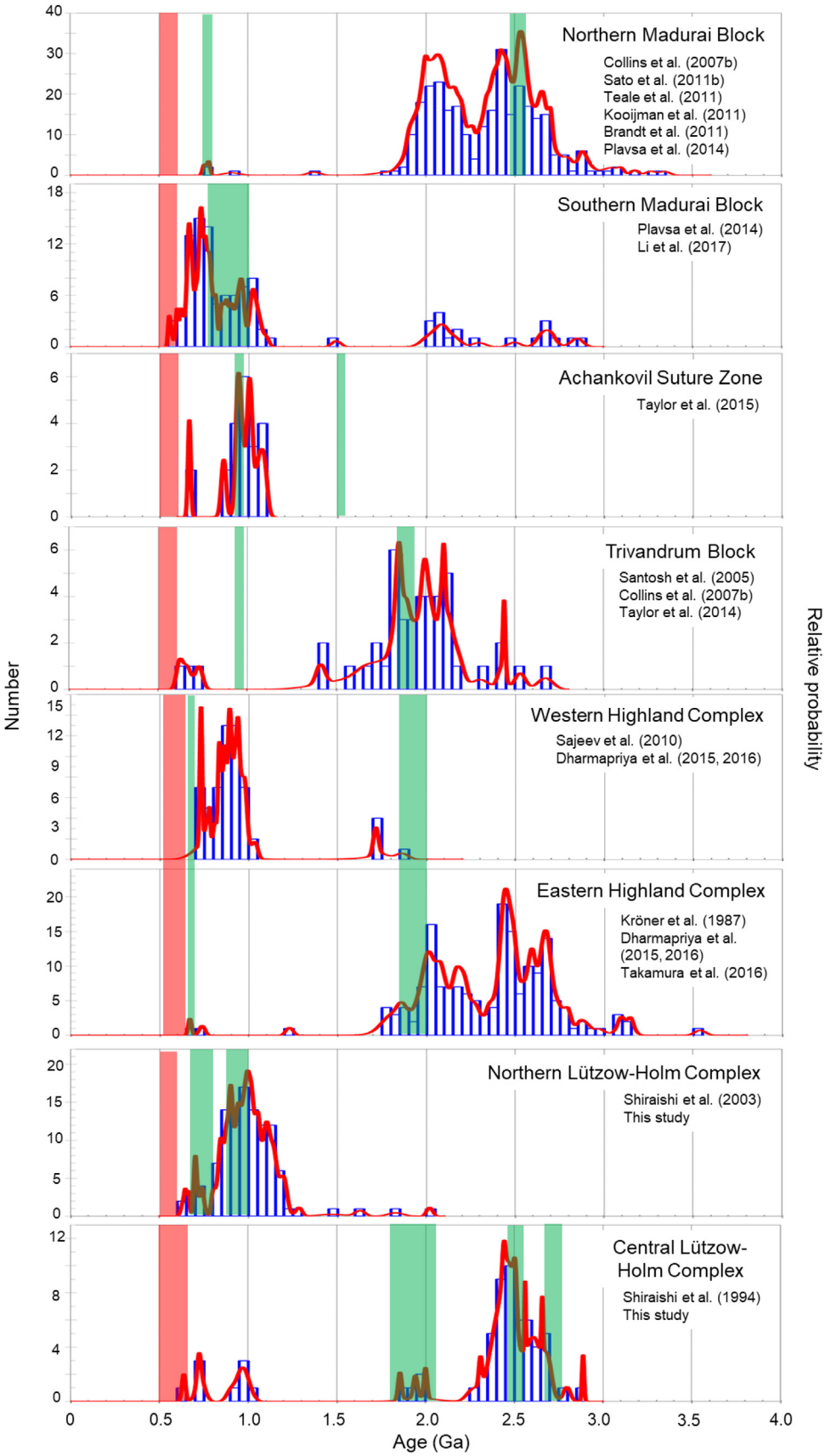

Figure 7. Histograms with probability density plots versus age (in Ga) of detrital zircon cores in the metasedimentary rocks from the northern and southern Madurai Block, Achankovil Suture Zone, and Trivandrum Block of southern India, the Highland Complex of Sri Lanka, and the LHC. Concordant (<10% discordance) detrital zircon ages were used to calculate the probability density plots. Older (>1.3 Ga) and younger (<1.3 Ga) ages are treated as $^{207}Pb/^{206}Pb$ and $^{206}Pb/^{238}U$ age, respectively, therefore some published papers that

our data from adjacent Langhovde region (ca. 1.2–0.8 Ga). Metasediments from Skallevikshalsen contain Neoarchean to Paleoproterozoic detrital zircons (ca. 2.8–1.8 Ga; Dunkley et al., 2014), although Paleoproterozoic grains are present but very minor in our sample (Fig. 5n). Our sample from Rundvågshetta does not contain detrital zircons, whereas Neoarchean (ca. 2.7–2.5 Ga) detrital zircon ages have been reported by Shiraishi et al. (1994) and Dunkley et al. (2014) from the region. Although we have no data from Telen in the central LHC, Neoproterozoic (ca. 1.0 Ga; Shiraishi et al., 1994) and Archean to Paleoproterozoic (ca. 2700, 2500 and 1800 Ma; Dunkley et al., 2014) detrital zircons were reported from the locality.

Dunkley et al. (2014) subdivided metasediments of the LHC into three types based on geochronological features: Syowa Paragneiss (ca. 1.0 Ga and 0.63 Ga), Skallen Supracrustals (ca. 2.5 Ga and 2.1–1.85 Ga), and Rundvåg Paragneiss (ca. 2.5 Ga). Predominant late Meso- to Neoproterozoic detrital zircon ages reported in this study from Sôya Coast are consistent with the Syowa Paragneiss, and our new ages indicate the occurrence of similar Meso- to Neoproterozoic detrital zircons from the northeastern part of the complex along Price Olav Coast (e.g., Tenmondai Rock and Akarui Point). On the other hand, metasediments with Neoarchean detrital zircons from the southwestern LHC (e.g., Skallevikshalsen) is comparable with the Rundvåg Paragneiss and Skallen Supracrustals, and our new data suggest that the ca. 2.5 Ga unit might continue to the western part of the LHC in Austhovde.

The late Neoproterozoic to Cambrian (619–486 Ma) metamorphic ages were obtained from structureless zircon grains and/or homogeneous rims, mantles, and rarely cores with lower Th/U ratios than detrital grains (Figs. 4 and 5, Supplementary Table 1). The results are consistent with previous studies that argued a late Neoproterozoic regional metamorphism in the LHC (e.g., Shiraishi et al., 1994, 2003, 2008; Asami et al., 1997; Hokada and Motoyoshi, 2006; Tsunogae et al., 2014, 2015, 2016; Kawakami et al., 2016). The depositional age of metasediments in the ca. 1.0 Ga northern LHC has been constrained as late Neoproterozoic (631–618 Ma) based on the youngest detrital zircon age (631 Ma from Akarui Point) and the oldest metamorphic age (618 Ma from West Ongul). We could not constrain the depositional age of the southwestern LHC because of lack of younger detrital zircons (Fig. 5).

6.2. Provenances of detrital zircons

6.2.1. Proximal sources

As summarized in geological background, three discrete magmatic suites have been reported from the LHC as follows. (1) Neoproterozoic (ca. 1.0–0.8 Ga) ages from Price Olav Coast (Cape Hinode, Niban Rock, Kasumi Rock, Akarui Point, Tama Point), northern Sôya Coast (Skarvsnes, West and East Ongul Island, Khuka), and Price Harald Coast (Innhovde, Hutatu Iwa) areas (Shiraishi et al., 1994; Dunkley et al., 2014; Tsunogae et al., 2015; Kazami et al., 2016). (2) Neoarchean (ca. 2.5 Ga) ages from the southwestern part of the complex (Rundvågshetta, Botnutten, Sudare Rock, Ongul, and Vesleknausen) (Shiraishi et al., 1994, 2008; Dunkley et al., 2014; Tsunogae et al., 2014, 2016). (3) Minor Paleoproterozoic (ca. 1.8 Ga) ages from Sôya and Prince Harald Coasts (Austhovde, Skallevikshalsen, Skallen, and Telen) (Dunkley et al., 2014; Takahashi et al., 2017). Such regional distribution of Neoproterozoic (ca. 1.0), Neoarchean (ca. 2.5), and Paleoproterozoic (ca. 1.8 Ga) magmatic suites in the northeastern, the southwestern, and the central parts of the LHC, respectively, is consistent with the distribution trend of detrital zircons in associated metasedimentary rocks discussed in this study. For example, ca. 1.2–0.7 detrital ages are dominant in Prince Olav Coast and northern Sôya Coast areas (Tenmondai Rock, West Ongul, Langhovde) where ca. 1.0 magmatic ages are abundantly reported (e.g., Tsunogae et al., 2015). Approximate 2.8–2.4 Ga detrital ages were obtained from the southern Lützow-Holm Bay area (Skallevikshalsen, Sudare Rock, Rundvågshetta) where ca. 2.5 Ga magmatic ages are reported. Therefore, it is logical that Neoproterozoic and Neoarchean detrital zircons discussed in this study could have been derived from adjacent terranes (Fig. 8a). The ca. 1.8 Ga Paleoproterozoic unit in Telen–Skallen–Skallevikshalsen–Austhovde region in the central LHC (Takahashi et al., 2017) could also be a provenance of 1.8 Ga detrital zircons from Telen reported by Dunkley et al. (2014). Therefore, most of the detrital zircon ages reported from the LHC can be explained by proximal transportation of zircon grains from adjacent magmatic suites in the LHC. Similar predominantly late Meso- to Neoproterozoic detrital zircons with subordinate Archean to Paleoproterozoic zircons are reported from the Sør Rondane Mountains (Kitano et al., 2016 and reference therein), suggesting similar provenances. Subsequent collision of the ca. 2.5 Ga microcontinent and ca. 1.0 Ga northern LHC–Vijayan Complex during latest Neoproterozoic to Cambrian (Takahashi et al., 2017) juxtaposed the accreted sediments with dominant ca. 1.0 Ga zircon in the north and ca. 2.5 Ga zircon in the south, forming the sedimentary unit in the central LHC (Fig. 8b).

It is important to note that there is no appropriate provenance for the late Mesoproterozoic (ca. 1.3–1.2 Ga) detrital zircons reported from Prince Olav Coast (e.g., 1212 Ma from Akarui Point) and northern Sôya (e.g., 1199 Ma from West Ongul, 1283 Ma from Langhovde, and similar ages reported in Dunkley et al., 2014) because of the lack of Mesoproterozoic protoliths. Therefore, although most of the detrital zircons could have been derived from proximal sources, at least some of them might have come from distal provenances in the adjacent Gondwana fragments.

6.2.2. Distal sources

Below we evaluate the possible provenances of late Mesoproterozoic (ca. 1.3–1.2 Ga) detrital zircons obtained from Prince Olav Coast and northern Sôya Coast areas. We also consider the possible sources of Neoproterozoic (ca. 1.0 Ga), Paleoproterozoic (ca. 2.1–1.8 Ga), and Neoarchean (ca. 2.5 Ga) detrital zircons in the LHC also. The Rayner Complex, exposed east of the LHC, is a typical example of early Neoproterozoic orogenic complex in East Antarctica, from which late Meso- to early Neoproterozoic (ca. 1380–900 Ma) magmatic ages have been reported (e.g., Fitzsimons, 2000; Kelly et al., 2002; Halpin et al., 2005; Boger, 2011; Grew et al., 2012; Liu et al., 2014). Similar ca. 1400–1000 Ma magmatic suites have also been reported from the Eastern Ghats Belt of India (e.g., Shaw et al., 1997). These Mesoproterozoic to early Neoproterozoic basement complexes could be one of the provenances of ca. 1.3–1.2 Ga detrital zircons in the northeastern LHC.

discuss only $^{207}Pb/^{206}Pb$ and $^{206}Pb/^{238}U$ ages are not argued here. Green and red bands indicate magmatic and metamorphic ages reported from each terrane, respectively. References of detrital zircon ages are shown in the figure. Magmatic and metamorphic ages of the Highland Complex and southern Indian terranes are cited from Dharmapriya et al. (2016) and references therein, and those of the LHC are cited from Shiraishi et al. (1994, 2003, 2008), Asami et al. (1997), Santosh et al. (2005), Hokada and Motoyoshi (2006), Dunkley (2007), Brandt et al. (2011), Kooijman et al. (2011), Sato et al. (2011b), Dunkley et al. (2014), Plavsa et al. (2014), Taylor et al. (2014), Tsunogae et al. (2014, 2015, 2016), Kazami et al. (2015), Taylor et al. (2015), Kawakami et al. (2016), Li et al. (2017).

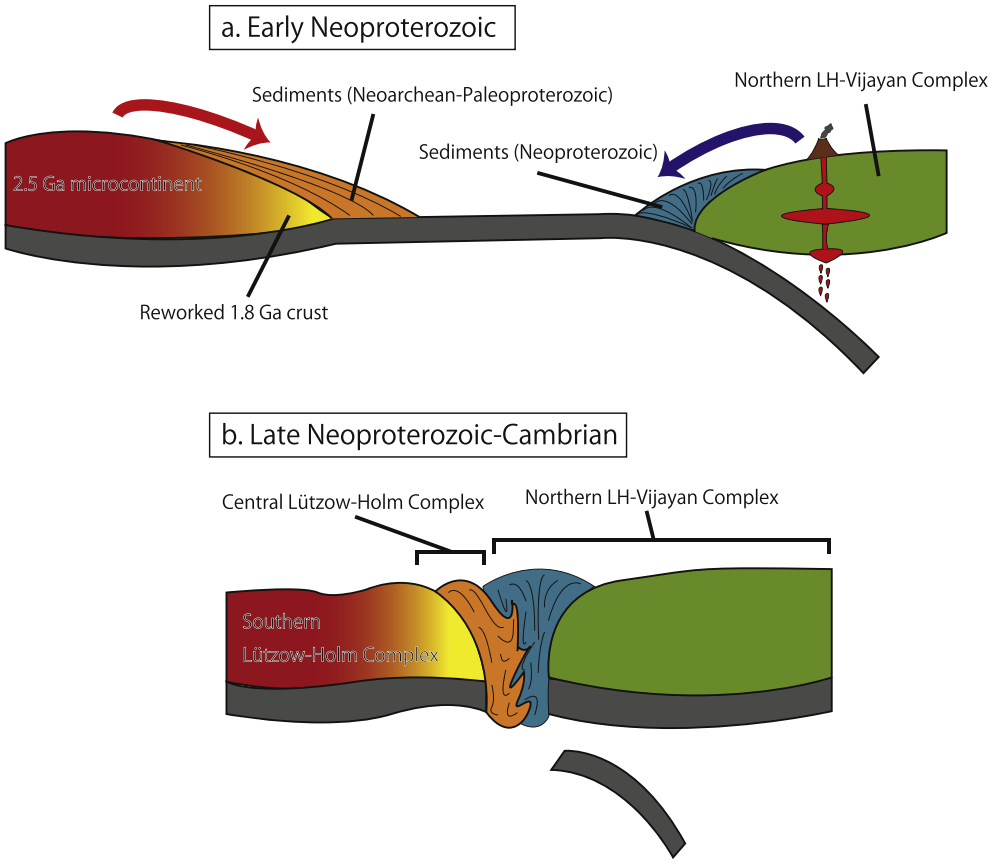

Figure 8. A schematic model illustrating geological and tectonic evolution of the LHC in (a) early Neoproterozoic and (b) late Neoproterozoic to Cambrian.

Early to middle Neoproterozoic magmatic rocks have been reported from some Gondwana fragments such as central-western Madagascar (ca. 1.0–0.8 Ga; e.g., Tucker et al., 2011), the Unango and Marrupa complexes of northern Mozambique (ca. 1.1–0.75 Ga; e.g., Bingen et al., 2009; Macey et al., 2010), the southern Madurai Block in southern India (ca. 1.0 Ga and 0.8 Ga; e.g., Plavsa et al., 2012; Santosh et al., 2017), and the basement rocks in Sri Lanka (ca. 1.0–0.73 Ga Wanni Complex (e.g., Santosh et al., 2014; He et al., 2016a), ca. 1.1–0.77 Ga Kadugannawa Complex (e.g., Kröner et al., 2003; Willbold et al., 2004; Santosh et al., 2014; He et al., 2016a), and ca. 1.1–1.0, 0.97–0.94, and 0.77–0.62 Ga Vijayan Complex (Kröner et al., 2003, 2013; He et al., 2016b; Ng et al., 2017)), which could be distal provenances of Neoproterozoic (ca. 1.0 Ga) detrital zircons in the LHC. The Yamato–Belgica Complex, exposed southwest of the LHC, shows early Neoproterozoic protolith ages (Shiraishi et al., 1994, 2003). The Sør Rondane Mountain and the central Dronning Maud Land of East Antarctica are also dominantly composed of early Neoproterozoic terranes (e.g., Shiraishi et al., 2008 and references therein). Jacobs et al. (2015) proposed early Neoproterozoic and juvenile oceanic magmatic arc affinities from the southeast Dronning Maud Land Province and defined the Tonian Oceanic Arc Super Terrane (TOAST). These early Neoproterozoic (ca. 1.0 Ga) magmatic suites can also have possibilities to be the provenances of Neoproterozoic detrital zircons in the LHC.

Neoarchean–Paleoproterozoic magmatic and metamorphic terranes, which could be sources of ca. 2.8–2.4 Ga detrital zircons in the southwestern LHC, have also been reported in several distal regions such as the western (ca. 3.4–2.9 and 2.8–2.5 Ga) and the eastern (ca. 2.5 Ga) Dharwar Craton (Beckinsale et al., 1980; Chadwick et al., 2000; Jayananda et al., 2000, 2006; Collins et al., 2003), Nilgiri Block (ca. 2.5 Ga; Samuel et al., 2014), Salem Block (ca. 2.7, 2.65, 2.5 Ga; Ghosh et al., 2004; Clark et al., 2009; Saitoh et al., 2011; Sato et al., 2011a; Anderson et al., 2012; Ram Mohan et al., 2013; Collins et al., 2014), and the northern Madurai Block (ca. 2.5 Ga; Teale et al., 2011; Plavsa et al., 2012; Collins et al., 2014) of southern India, the Napier Complex of East Antarctica (ca. 3.8, 3.0, 2.8, 2.5 Ga; Harley and Black, 1997), and the Antongil Block of eastern Madagascar (ca. 3.3–3.1 and 2.7–2.5 Ga; Schofield et al., 2010). Similar Neoarchean to Paleoproterozoic basements are also distributed in the Congo–Tanzania–Bangweulu Block of east and central Africa, such as the Tanzania Craton (ca. 2.7 Ga; Borg and Krogh, 1999; Collins et al., 2004) and Usagaran–Ubendian belt (ca. 2.3–1.8 Ga; e.g., Lenoir et al., 1994; Collins et al., 2004, 2007b; Collins and Pisarevsky, 2005), although the regions might be bit far from East Antarctica during Neoproterozoic.

6.3. Implications for Antarctica–Sri Lanka correlation

For the correlation of detrital zircon ages from the LHC and Sri Lanka, first we briefly summarize the available detrital zircon ages from the Highland Complex. The dominant population of detrital zircons in the eastern part of the Highland Complex is Paleoarchean to Paleoproterozoic (ca. 3.5–1.7 Ga; Fig. 7) (Kröner et al., 1987; Hölzl et al., 1994; Dharmapriya et al., 2016; Takamura et al., 2016), whereas younger early to middle Neoproterozoic (ca. 1.0–0.7 Ga) ages were obtained from the western Highland Complex near the boundary with the Kadugannawa Complex (Sajeev et al., 2010; Dharmapriya et al., 2015, 2016). Kitano et al. (2015a, b) reported predominant Paleo- to early Mesoproterozoic (ca. 2.0–1.5 Ga) detrital zircon ages from the eastern part of the Highland Complex,

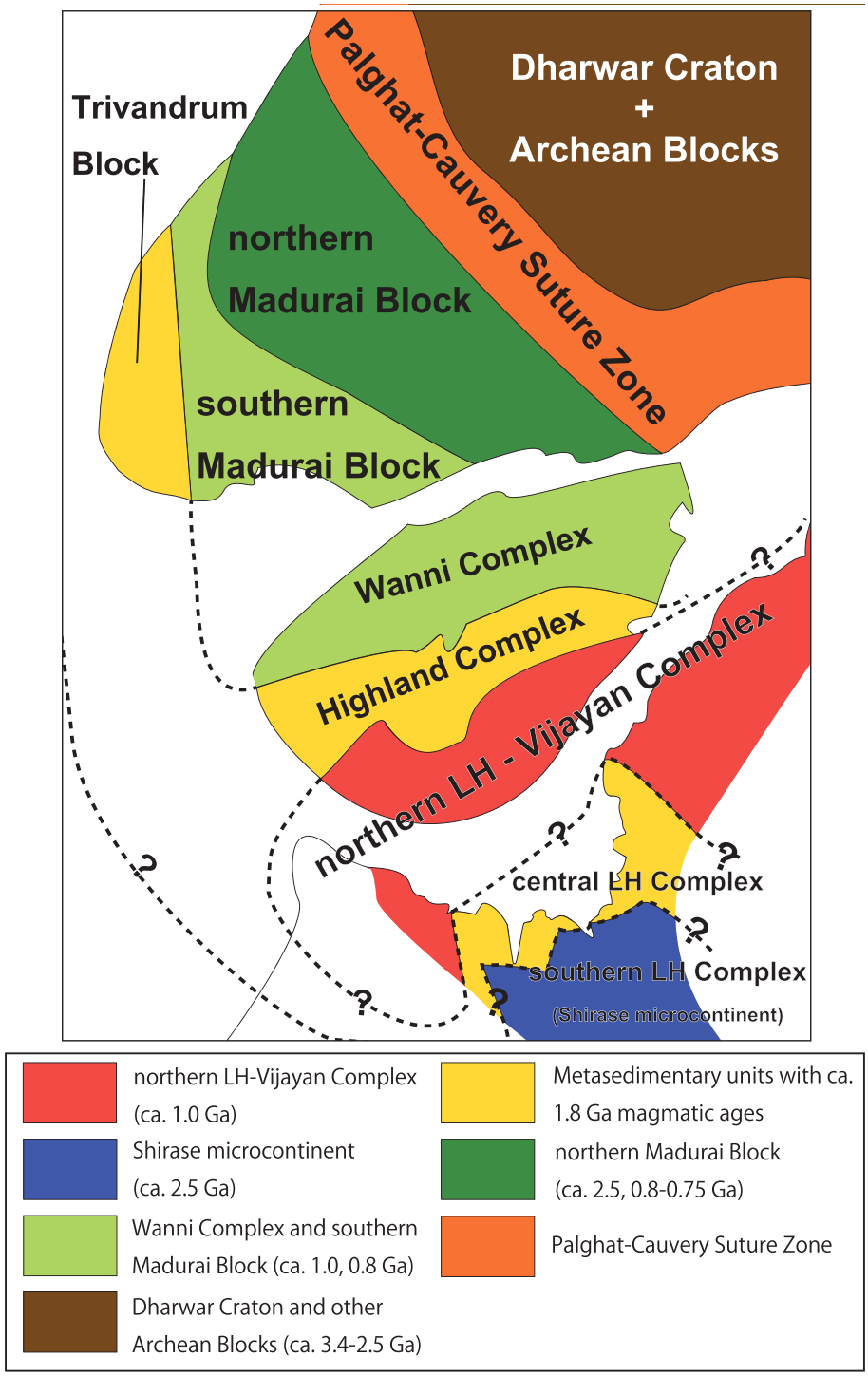

Figure 9. A generalized geological framework of Sri Lanka, southern India, and the Lützow–Holm Complex showing the distribution and continuation of metasedimentary units (modified after Takahashi et al., 2017). The continuation of the Trivandrum Block and the Highland Complex is based on previous studies (e.g., Dharmapriya et al., 2016).

and predominant early to middle Neoproterozoic ages (ca. 1.0–0.7 Ga) from the western part (Fig. 7).

The metasedimentary unit with Paleoarchean to Paleoproterozoic (ca. 3.5–1.7 Ga) detrital zircon ages from the eastern Highland Complex are consistent with those from Austhovde (2.5–2.4 Ga, this study), Skallevikshalsen (2.8–2.5 Ga, this study; 2.8–1.8 Ga, Dunkley et al., 2014), Telen (3.3–2.5 and 1.8 Ga, Dunkley et al., 2014), and Rundvågshetta (3.2–2.5 Ga; Shiraishi et al., 1994; Dunkley et al., 2014), which are grouped as Rundvåg Paragneiss (Fig. 7). In addition, Neoproterozoic detrital zircons from the western Highland Complex (Sajeev et al., 2010; Dharmapriya et al., 2015, 2016; Kitano et al., 2015a, b) and the Showa Paragneiss in the northern LHC (this study and Dunkley et al., 2014) are also comparable. Based on the occurrences of similar metasedimentary

units with abundant Neoarchean–Paleoproterozoic and Neoproterozoic detrital zircons, it is logical that the Highland Complex and the metasedimentary unit in the LHC have similar provenances, suggesting that the Highland Complex could be a direct continuation of the metasedimentary unit of the LHC. This model is consistent with the lithological, structural, geochronological, and tectonothermal similarities of the two regions reported in previous studies (e.g., Yoshida et al., 1992; Shiraishi et al., 1994; Kriegsman, 1995; Osanai et al., 2016a, b; Takamura et al., 2016).

In contrast, Takahashi et al. (2017) argued that, although the Highland Complex and the metasedimentary unit of the LHC could have formed through similar convergent tectonics defining suture zones, the Highland Complex does not directly continue to the LHC because the metasedimentary unit in the LHC was formed by single-sided subduction of oceanic plate beneath the Neoproterozoic arc (northern LH–Vijayan Complex) and subsequent collision with ca. 2.5 Ga microcontinent (Shirase microcontinent), whereas the Highland Complex was formed by double-sided subduction and collision of the Neoproterozoic Wanni and Vijayan arcs in late Neoproterozoic (Santosh et al., 2014; He et al., 2016b). They regarded that two metasedimentary units are discrete suture zones separated by the northern LH–Vijayan Complex. Based on the detrital zircon data presented in this study, we revise Takahashi et al. (2017) model and infer that the Highland Complex and metasedimentary unit of the LHC might be part of a unified latest Neoproterozoic suture zone which includes a large block of northern LH–Vijayan Complex as a remnant of ca. 1.0 Ga magmatic arc (Fig. 9). Previous studies pointed out the continuation of the Trivandrum Block in southern India and the Highland Complex. For example, Kröner et al. (2012) showed a reconstruction model that juxtaposes the Trivandrum Block and the Highland Complex based on their lithological similarities (khondalite, lenses of mafic granulite, and charnockite) and geochronology of detrital zircons (Paleoproterozoic). Dharmapriya et al. (2016) also pointed out geochronological similarities between the Trivandrum Block and the Highland Complex based on Paleoproterozoic (ca. 2000–1800 Ma) magmatic zircon ages, Neoarchean to Neoproterozoic (ca. 2800–700 Ma) detrital zircon/monazite ages, and late Neoproterozoic to Cambrian (ca. 665–500 Ma) metamorphic zircon ages. Thus, we conclude that both the metasedimentary units in the LHC and the Highland Complex might continue to the Trivandrum Block.

7. Conclusions

(1) The age distributions of detrital zircons in metasediments from the LHC show variations within the complex; Neoproterozoic ages (1.1–0.63 Ga) from the northeastern LHC and Neoarchean to Paleoproterozoic ages (2.8–2.4 Ga) from the southwestern LHC.

(2) Late Neoproterozoic to Cambrian ages (ca. 600–500 Ma) obtained from zircon rims and homogeneous grains probably indicate the timing of high-grade metamorphism. Based on the age of the youngest detrital zircon as well as the oldest metamorphic age, the depositional age of sediments in the northeastern LHC can be well constrained at 630–600 Ma, whereas that of the southwestern LHC remains unknown.

(3) Late Mesoproterozoic to Neoproterozoic (ca. 1.0 Ga) and Neoarchean to Paleoproterozoic (ca. 2.5 Ga) magmatic suites in the LHC could be proximal provenances of the detrital zircons in the northeastern and southwestern LHC, respectively. Subordinate middle to late Mesoproterozoic (1.3–1.2 Ga) detrital zircons obtained from Akarui Point and Langhovde could have been derived from adjacent Gondwana fragments (e.g., Rayner Complex, Eastern Ghats Belt). For the explanation of minor ~2.8 Ga detrital zircons from Skallevikshalsen, distal sources such as Paleo- to Mesoarchean domains in India, Africa, and Antarctica should be also considered.

(4) The detrital zircons from the Highland Complex of Sri Lanka show similar Neoarchean to Paleoproterozoic (ca. 2.5 Ga) and Neoproterozoic (ca. 1.0 Ga) ages, which are comparable with those of the LHC, suggesting that the two regions (suture zones) might have formed under similar convergent tectonics. We regard that the Highland Complex and metasedimentary unit of the LHC form a unified latest Neoproterozoic suture zone which includes a large block of northern LH–Vijayan Complex as a remnant of ca. 1.0 Ga magmatic arc. Both the metasedimentary units in the LHC and the Highland Complex might continue to the Trivandrum Block in southern India.

Acknowledgment

We thank Profs. K. Shiraishi, Y. Motoyoshi, T. Kawasaki, Y. Osanai, Y. Hiroi, Drs. T. Hokada, D.J. Dunkley, T. Miyamoto, M. Kato, and all JARE-52 members for their support of geological field work and discussion. We also thank National Museum of Nature and Science for analytical facilities and support. Two anonymous reviewers provided valuable comments and suggestions to the earlier version of this manuscript. We also thank Guest Editor Dr. Qiong-Yan Yang for her editorial comments. This study was partly supported by a Grant-in-Aid for Scientific Research (B) from Japan Society for the Promotion of Science (JSPS) (No. 26302009) and by the NIPR General Collaboration Projects (No. 26-34) to Tsunogae.

Appendix A. Supplementary data

Supplementary data related to this article can be found at http://dx.doi.org/10.1016/j.gsf.2017.08.006.

References

Anderson, J.R., Payne, J.L., Kelsey, D.E., Hand, M., Collins, A.S., Santosh, M., 2012. High-pressure granulites at the dawn of the Proterozoic. Geology 40, 431–434.

Asami, M., Suzuki, K., Adachi, M., 1997. Th, U and Pb analytical data and CHIME dating of monazites from metamorphic rocks of the Rayner, Lützow-Holm, Yamato-Belgica and Sør Rondane Complexes, East Antarctica. Proceedings of the NIPR Symposium on Antarctic Geosciences 10, 130–152.

Beckinsale, R.D., Drury, S.A., Holt, R.W., 1980. 3,360-Myr old gneisses from the South Indian Craton. Nature 283, 469–470.

Bingen, B., Jacobs, J., Viola, G., Henderson, I.H.C., Skår, Ø., Boyd, R., Thomas, R.J., Solli, A., Key, R.M., Daudi, E.X.F., 2009. Geochronology of the Precambrian crust in the Mozambique belt in NE Mozambique, and implications for Gondwana assembly. Precambrian Research 170, 231–255.

Boger, S.D., 2011. Antarctica – before and after Gondwana. Gondwana Research 19, 335–371.

Borg, G., Krogh, T., 1999. Isotopic data of single zircons from the Archaean Sukumaland Greenstone Belt, Tanzania. Journal of African Earth Sciences 29, 310–312.

Brandt, S., Schenk, V., Raith, M.M., Appel, P., Gerdes, A., Srikantappa, C., 2011. Late Neoproterozoic P-T evolution of HP-UHT granulites from the Palani Hills (South India): new constraints from phase diagrammodelling, LA-ICP-MS zircon dating and in-situ EMP monazite dating. Journal of Petrology 52, 1813–1856.

Cawood, P.A., Nemchin, A.A., Freeman, M., Sircombe, K., 2003. Linking source and sedimentary basin: detrital zircon record of sediment flux along a modern river system and implications for provenance studies. Earth and Planetary Science Letters 210, 259–268.

Chadwick, B., Vasudev, V.N., Hegde, G.V., 2000. The Dharwar craton, southern India, interpreted as the result of Late Archaean oblique convergence. Precambrian Research 99, 91–111.

Clark, C., Collins, A.S., Timms, N.E., Kinny, P.D., Chetty, T.R.K., Santosh, M., 2009. SHRIMP U–Pb age constraints on magmatism and high-grade metamorphism in the Salem Block, southern India. Gondwana Research 16, 27–36.

Collins, A.S., Pisarevsky, S.A., 2005. Amalgamating eastern Gondwana: the evolution of the Circum-Indian Orogens. Earth Science Review 71, 229–270.

Collins, A.S., Kröner, A., Fitzsimons, I.C.W., Razakamanana, T., 2003. Detrital footprint of the Mozambique Ocean: U/Pb SHRIMP and Pb evaporation zircon geochronology of metasedimentary gneisses in Eastern Madagascar. Tectonophysics 375, 77–99.
Collins, A.S., Reddy, S.M., Buchan, C., Mruma, A., 2004. Temporal constraints on palaeoproterozoic eclogite formation and exhumation (Usagaran Orogen, Tanzania). Earth Planetary Science Letters 224, 175–192.
Collins, A.S., Clark, C., Sajeev, K., Santosh, M., Kelsey, D.E., Hand, M., 2007a. Passage through India: the Mozambique Ocean suture, high pressure granulites and the Palghat-Cauvery Shear System. Terra Nova 19, 141–147.
Collins, A.S., Santosh, M., Braun, I., Clark, C., 2007b. Age and sedimentary provenance of the Southern Granulites, South India: U–Th–Pb SHRIMP secondary ion mass spectrometry. Precambrian Research 155, 125–138.
Collins, A.S., Clark, C., Plavsa, D., 2014. Peninsular India in Gondwana: the tectonothermal evolution of the Southern Granulite Terrain and its Gondwanan counterparts. Gondwana Research 25, 190–203.
Dharmapriya, P.L., Malaviarachchi, S.P.K., Santosh, M., Tang, L., Sajeev, K., 2015. Late-Neoproterozoic ultrahigh-temperature metamorphism in the Highland Complex, Sri Lanka. Precambrian Research 271, 311–333.
Dharmapriya, P.L., Malaviarachchi, S.P.K., Sajeev, K., Zhang, C., 2016. New LA-ICP-MS U-Pb ages of detrital zircons from the Highland Complex: insights into Late Cryogenian to Early Cambrian (ca. 665-535 Ma) linkage between Sri Lanka and India. International Geology Review 58, 1856–1883.
Dunkley, D.J., 2007. Isotopic zonation in zircon as a recorder of progressive metamorphism. Goldschmidt Conference Abstracts Geochimica et Cosmochimica Acta A224.
Dunkley, D.J., Shiraishi, K., Motoyoshi, Y., Tsunogae, T., Miyamoto, T., Hiroi, Y., Carson, C.J., 2014. Deconstructing the Lützow-Holm Complex with Zircon Geochronology. Abstract of 7th international SHRIMP workshop program, pp. 116–121.
Eggins, S.M., Kinsley, L.P.J., Shelley, J.M.G., 1998. Deposition and element fractionation processes of occurring during atmospheric pressure sampling for analysis by ICP-MS. Applied Surface Science 129, 278–286.
Fitzsimons, I.C.W., 2000. Grenville-age basement provinces in East Antarctica: evidence for three separate collisional orogens. Geology 28, 879–882.
Fraser, G., McDougall, I., Ellis, D.J., Williams, I.S., 2000. Timing and rate of isothermal decompression in Pan-African granulites from Rundvågshetta, East Antarctica. Journal of Metamorphic Geology 18, 441–454.
Gebauer, D., Williams, I.S., Compston, W., Grünenfelder, M., 1989. The development of the Central European continental crust since the Early Archaean based on conventional and ion-microprobe dating of up to 3.84 b.y. old detrital zircons. Tectonophysics 157, 81–96.
Ghosh, J.G., de Wit, M.J., Zartman, R.E., 2004. Age and tectonic evolution of Neoproterozoic ductile shear zones in the Southern Granulite Terrain of India, with implications for Gondwana studies. Tectonics 23 (TC3006).
Grew, G., Carson, C.J., Christy, A.G., Maas, R., Yaxley, G.M., Boger, S., Fanning, C.M., 2012. New constraints from U–Pb, Lu–Hf and Sm–Nd isotopic data on the timing of sedimentation and felsic magmatism in the Larsemann Hills, Prydz Bay, East Antarctica. Precambrian Research 206–207, 87–108.
Halpin, J.A., Gerakiteys, C.L., Clarke, G.L., Belousova, E.A., Griffin, W.L., 2005. In-situ U–Pb geochronology and Hf isotope analyses of the Rayner Complex, east Antarctica. Contributions to Mineralogy and Petrology 148, 689–706.
Harley, S.L., Black, L.P., 1997. A revised Archaean chronology for the Napier Complex, Enderby Land, from SHRIMP ion-microprobe studies. Antarctic Science 9, 74–91.
He, X.F., Santosh, M., Tsunogae, T., Malaviarachchi, S.P.K., 2016a. Early to late Neoproterozoic magmatism and magma mixing – mingling in Sri Lanka: implications for convergent margin processes during Gondwana assembly. Gondwana Research 32, 151–180.
He, X.-F., Santosh, M., Tsunogae, T., Malaviarachchi, S.P.K., Dharmapriya, P.L., 2016b. Neoproterozoic arc accretion along the 'eastern suture' in Sri Lanka during Gondwana assembly. Precambrian Research 279, 57–80.
Hiroi, Y., Shiraishi, K., Nakai, Y., Kano, T., Yoshikura, S., 1983. Geology and petrology of Prince Olav Coast, East Antarctica. In: Oliver, R.L., James, P.R., Jago, J.B. (Eds.), Antarctic Earth Science. Australian Academy of Science, Canberra, pp. 32–35.
Hiroi, Y., Shiraishi, K., Motoyoshi, Y., 1991. Late Proterozoic paired metamorphic complexes in East Antarctica, with special reference to the tectonic significance of ultramafic rocks. In: Thomson, M.R.A., Crame, J.A., Thomson, J.W. (Eds.), Geological Evolution of Antarctica. Cambridge University Press, Cambridge, pp. 83–87.
Hokada, T., Motoyoshi, Y., 2006. Electron microprobe technique for U–Th–Pb and REE chemistry of monazite, and its implications for pre-, peak- and post-metamorphic events of the Lützow-Holm Complex and the Napier Complex, East Antarctica. Polar Geoscience 19, 118–151.
Hölzl, S., Hofmann, A.W., Todt, W., Köhler, H., 1994. U–Pb Geochronology of the SriLankan basement. Precambrian Research 66, 123–149.
Iwamura, S., Tsunogae, T., Kato, M., Koizumi, T., Dunkley, D.J., 2013. Petrology and phase equilibrium modeling of spinel-sapphirine-bearing mafic granulite from Akarui Point, Lützow-Holm Complex, East Antarctica: implications for the *P-T* path. Journal of Mineralogical and Petrological Sciences 108, 345–350.
Jacobs, J., Thomas, R.J., 2004. Himalayan-type indenter-escape tectonics model for the southern part of the late Neoproterozoic-early Paleozoic East African-Antarctic orogeny. Geology 32, 721–724.
Jacobs, J., Elburg, M., Läufer, A., Kleinhanns, I.C., Henjes-Kunst, F., Estrada, S., Ruppel, A.S., Damaske, D., Montero, P., Bea, F., 2015. Two distinct Late Mesoproterozoic/Early Neoproterozoic basement provinces in central/eastern Dronning Maud Land, East Antarctica: the missing link, 15-21°E. Precambrian Research 265, 249–272.
Jayananda, M., Moyen, J.F., Martin, H., Peucat, J.J., Auvray, B., Mahabaleswar, B., 2000. Late Archaean (2550–2520 Ma) juvenile magmatism in the Eastern Dharwar craton, southern India: constraints from geochronology, Nd–Sr isotopes and whole rock geochemistry. Precambrian Research 99, 225–254.
Jayananda, M., Chardon, D., Peucat, J.J., Capdevila, R., 2006. 2.61 Ga potassic granites and crustal reworking in the western Dharwar craton, southern India: tectonic, geochronologic and geochemical constraints. Precambrian Research 150, 1–26.
Kawakami, T., Grew, E.S., Motoyoshi, Y., Shearer, C.K., Ikeda, T., 2008. Kornerupine sensu stricto associated with mafic and ultramafic rocks in the Lützow-Holm Complex at Akarui Point, East Antarctica: what is the source of boron? Geological Society, London, Special Publication 308, 351–375.
Kawakami, T., Hokada, T., Sakata, S., Hirata, T., 2016. Possible polymetamorphism and brine infiltration recorded in the garnet–sillimanite gneiss, Skallevikshalsen, Lützow–Holm Complex, East Antarctica. Journal of Mineralogical and Petrological Sciences 111, 129–143.
Kawano, Y., Nishi, N., Kagami, H., 2006. Rb-Sr and Sm-Nd mineral isochron ages of a pegmatitic gneiss from Oku-iwa Rock, Lützow-Holm Complex, East Antarctica. Polar Geoscience 19, 109–117.
Kawasaki, T., Nakano, N., Osanai, Y., 2011. Osumilite and a spinel + quartz association in garnet-sillimanite gneiss from Rundvågshetta, Lützow-Holm Complex, East Antarctica. Gondwana Research 19, 430–445.
Kazami, S., Tsunogae, T., Santosh, M., Tsutsumi, Y., Takamura, Y., 2016. Petrology, geochemistry and zircon U–Pb geochronology of a layered igneous complex from Akarui Point in the Lützow-Holm Complex, East Antarctica: implications for Antarctica-Sri Lanka correlation. Journal of Asian Earth Sciences 130, 206–222.
Kelly, N.M., Clarke, G.L., Fanning, C.M., 2002. A two-stage evolution of the Neoproterozoic Rayner Structural Episode: new U–Pb sensitive high resolution ionmicroprobe constraints from the Oygarden Group, Kemp Land, East Antarctica. Precambrian Research 116, 307–330.
Kitano, I., Osanai, Y., Nakano, N., Adachi, T., 2015a. LA-ICP-MS Zircon U–Pb Ages from Metamorphic Rocks in the Southwestern Part of Highland Complex, Sri Lanka. Abstract Volume, Japan Geoscience Union Meeting 2015, SMP09–P03.
Kitano, I., Osanai, Y., Nakano, N., Adachi, T., 2015b. LA-ICP-MS Zircon U–Pb Ages of High Temperature Metamorphic Rocks from the Western and Eastern Highland Complexes, Sri Lanka. Abstract Volume, 2015 Annual Meeting of Japan Association of Mineralogical Sciences, R8–01, p. 193 (in Japanese).
Kitano, I., Osanai, Y., Nakano, N., Adachi, T., 2016. Detrital zircon provenances for metamorphic rocks from southern Sør Rondane Mountains, East Antarctica: a new report of Archean to Mesoproterozoic zircons. Journal of Mineralogical and Petrological Sciences 111, 118–128.
Kooijman, E., Upadhyay, D., Mezger, K., Raith, M.M., Berndt, J., Srikantappa, C., 2011. Response of the U-Pb chronometer and trace elements in zircon to ultrahigh-temperature metamorphism: the Kadavur anorthosite complex, southern India. Chemical Geology 290, 177–188.
Kriegsman, L., 1995. The Pan-African events in East Antarctica: a review from Sri-Lanka and the Mozambique Belt. Precambrian Research 75, 263–277.
Kröner, A., Williams, I.S., Compston, W., Baur, N., Vitanage, P.W., Perera, L.R.K., 1987. Zircon ion microprobe dating of high grade rocks in Sri Lanka. Journal of Geology 95, 775–791.
Kröner, A., Kehelpannala, K.V.W., Hegner, A., 2003. Ca. 750–1100 Ma magmatic events and Grenville-age deformation in Sri Lanka: relevance for Rodinia supercontinent formation and dispersal, and Gondwana amalgamation. Journal of Asian Earth Sciences 22, 279–300.
Kröner, A., Santosh, M., Wong, J., 2012. Zircon ages and Hf isotopic systematics reveal vestiges of Mesoproterozoic to Archaean crust within the late Neoproterozoic-Cambrian high-grade terrain of southernmost India. Gondwana Research 21, 876–886.
Kröner, A., Rojas-Agramonte, Y., Kehelpannala, K.V.W., Zack, T., Hegner, E., Geng, H.Y., Wong, J., Barth, M., 2013. Age, Nd–Hf isotopes, and geochemistry of the Vijayan Complex of eastern and southern Sri Lanka: a Grenville-age magmatic arc of unknown derivation. Precambrian Research 234, 288–321.
Kuznetsov, N.B., Meert, J.G., Romanyuk, T.V., 2014. Ages of detrital zircons (U/Pb, LA-ICP-MS) from the Latest Neoproterozoic-Middle Cambrian (?) Asha Group and Early Devonian Takaty Formation, the Southwestern Urals: a test of an Australia-Baltica connection within Rodinia. Precambrian Research 244, 288–305.
Lenoir, J.L., Liégeois, J.P., Theunissen, K., Klerkx, J., 1994. The Palaeoproterozoic Ubendian shear belt in Tanzania: geochronology and structure. Journal of African Earth Sciences 19, 169–184.
Li, S.S., Santosh, M., Indu, G., Shaji, E., Tsunogae, T., 2017. Detrital zircon geochronology of quartzites from the southern Madurai Block, India: implications for Gondwana reconstruction. Geoscience Frontiers 8, 851–867.
Liu, X., Jahn, B.-M., Yue, Z., Jian, L., Ren, L., 2014. Geochemistry and geochronology of Mesoproterozoic basement rocks from the eastern Amery Ice Shelf and southwestern Prydz Bay, East Antarctica: implications for a long-lived

magmatic accretion in a continental arc. American Journal of Science 314, 508–547.
Ludwig, K.R., 2008. User's Manual for Isoplot 3.70. Berkeley Geochronology Center Special Publication, No. 4, p. 70.
Macey, P.H., Thomas, R.J., Grantham, G.H., Ingram, B.A., Jacobs, J., Armstrong, R.A., Roberts, M.P., Bingen, B., Hollick, L., de Kock, G.S., Viola, G., Bauer, W., Gonzales, E., Bjerkgård, T., Henderson, I.H.C., Sandstad, J.S., Cronwright, M.S., Harley, S., Solli, A., Nord gulen, Ã., Motuza, G., Daudi, E., Manhiça, V., 2010. Mesoproterozoic geology of the Nampula Block, northern Mozambique: tracing fragments of Mesoproterozoic crust in the heart of Gondwana. Precambrian Research 182, 124–148.
Meert, J., 2003. A synopsis of events related to the assembly of eastern Gondwana. Tectonophysics 362, 1–40.
Meert, J.G., Lieberman, B.S., 2008. The Neoproterozoic assembly of Gondwana and its relationship to the Ediacaran-Cambrian radiation. Gondwana Research 14, 5–21.
Nakamura, A., Kitamura, M., Kawakami, T., 2013. Microstructural records of multiple retrograde local H_2O supplement in the pelitic gneiss, Lützow-Holm Complex at Akarui Point, East Antarctica. Mineralogy and Petrology 108, 177–186.
Ng, S.W.P., Whitehouse, M.J., Tam, T.P.Y., Jayasingha, P., Wong, J.P.M., Denyszyn, S.W., Yiu, J.S.Y., Chang, S.C., 2017. Ca. 820–640 Ma SIMS U-Pb age signal in the peripheral Vijayan Complex, Sri Lanka: identifying magmatic pulses in the assembly of Gondwana. Precambrian Research 294, 244–256.
Nogi, Y., Jokat, W., Kitada, K., Steinhage, D., 2013. Geological structures inferred from airborne geophysical surveys around Lützow-Holm Bay, East Antarctica. Precambrian Research 234, 279–287.
Osanai, Y., Toyoshima, T., Owada, M., Tsunogae, T., Hokada, T., Crowe, W.A., Ikeda, T., Kawakami, T., Kawano, Y., Kawasaki, T., Ishikawa, M., Motoyoshi, Y., Shiraishi, K., 2004. Explanatory Text of Geological Map of Skallen, Antarctica (Revised Edition). In: Antarctic Geological Map Series, Sheet 39 Skallen (Revised Edition). National Institute of Polar Research, Japan.
Osanai, Y., Sajeev, K., Nakano, N., Kitano, I., Kehelpannala, W.K., Adachi, T., Malaviarachchi, S.P., 2016a. UHT granulites of the Highland Complex, Sri Lanka I: geological and petrological background. Journal of Mineralogical and Petrological Sciences 111, 145–156.
Osanai, Y., Sajeev, K., Nakano, N., Kitano, I., Kehelpannala, W.K., Adachi, T., Malaviarachchi, S.P., 2016b. UHT granulites of the Highland Complex, Sri Lanka II: geochronological constraints and implications for Gondwana correlation. Journal of Mineralogical and Petrological Sciences 111, 157–169.
Paces, J.B., Miller, J.D., 1993. Precise U–Pb ages of Duluth Complex and related mafic intrusions, northeastern Minnesota: geochronological insights to physical, petrogenetic, paleomagnetic and tectonomagmatic processes associated with the 1.1 Ga midcontinent rift system. Journal of Geophysical Research 98, 13997–14013.
Plavsa, D., Collins, A.S., Foden, J.F., Kropinski, L., Santosh, M., Chetty, T.R.K., Clark, C., 2012. Delineating crustal domains in Peninsular India: age and chemistry of orthopyroxene-bearing felsic gneisses in the Madurai Block. Precambrian Research 198–199, 77–93.
Plavsa, D., Collins, A.S., Payne, J.L., Foden, J.D., Clark, C., Santosh, M., 2014. Detrital zircons in basement metasedimentary protoliths unveil the origins of southern India. Geological Society of America Bulletin 126, 791–812.
Ram Mohan, M., Satyanarayanan, M., Santosh, M., Sylvester, P.J., Tubrett, M., Lam, R., 2013. Neoarchean suprasubduction zone arc magmatism in southern India: geochemistry, zircon U–Pb geochronology and Hf isotopes of the Sittampundi Anorthosite Complex. Gondwana Research 23, 539–557.
Saitoh, Y., Tsunogae, T., Santosh, M., Chetty, T.R.K., Horie, K., 2011. Neoarchean high-pressure metamorphism from the northern margin of the Palghat-Cauvery Suture Zone, southern India: petrology and zircon SHRIMP geochronology. Journal of Asian Earth Sciences 42, 268–285.
Sajeev, K., Williams, I.S., Osanai, Y., 2010. Sensitive high-resolution ion microprobe U–Pb dating of prograde and retrograde ultrahigh-temperature metamorphism as exemplified by Sri Lankan granulites. Geology 38, 971–974.
Samuel, V.O., Santosh, M., Liu, S., Wang, W., Sajeev, K., 2014. Neoarchean continental growth through arc magmatism in the Nilgiri Block, southern India. Precambrian Research 245, 146–173.
Santosh, M., Collins, A.S., Morimoto, T., Yokoyama, K., 2005. Depositional constraints and age of metamorphism in southern India: U–Pb chemical (EPMA) and isotopic (SIMS) ages from the Trivandrum Block. Geological Magazine 142, 255–268.
Santosh, M., Maruyama, S., Sato, K., 2009. Anatomy of a Cambrian suture in Gondwana: pacific-type orogeny in southern India? Gondwana Research 16, 321–341.
Santosh, M., Tsunogae, T., Malaviarachchi, S.P.K., Zhang, Z., Ding, H., Tang, L., Dharmapriya, P.L., 2014. Neoproterozoic crustal evolution in Sri Lanka: insights from petrologic, geochemical and zircon U–Pb and Lu–Hf isotopic data and implications for Gondwana assembly. Precambrian Research 255, 1–29.
Santosh, M., Yang, Q.Y., Shaji, E., Tsunogae, T., Ram Mohan, M., Satyanarayanan, M., 2015. An exotic Mesoarchean microcontinent: the Coorg Block, southern India. Gondwana Research 27, 165–195.
Santosh, M., Yang, Q.Y., Shaji, E., Mohan, M.R., Tsunogae, T., Satyanarayanan, M., 2016. Oldest rocks from Peninsular India: evidence for Hadean to Neoarchean crustal evolution. Gondwana Research 29, 105–135.
Santosh, M., Hu, C.-N., He, X.-F., Li, S.-S., Tsunogae, T., Shaji, E., Indu, G., 2017. Neoproterozoic arc magmatism in the southern Madurai Block, India: subduction, relamination, continental outbuilding, and the growth of Gondwana. Gondwana Research 45, 1–42.
Sato, K., Santosh, M., Tsunogae, T., Chetty, T.R.K., Hirata, T., 2011a. Laser ablation ICP mass spectrometry for zircon U–Pb geochronology of metamorphosed granite from the Salem Block: implication for Neoarchean crustal evolution in southern India. Journal of Mineralogical and Petrological Sciences 106, 1–12.
Sato, K., Santosh, M., Tsunogae, T., Chetty, T.R.K., Hirata, T., 2011b. Subduction–accretion-collision history along the Gondwana suture in southern India: a laser ablation ICP-MS study of zircon chronology. Journal of Asian Earth Sciences 40, 162–171.
Schofield, D.I., Thomas, R.J., Goodenough, K.M., De Waele, B., Pitfield, P.E.J., Key, R.M., Bauer, W., Walsh, G.J., Lidke, D.J., Ralison, A.V., Rabarimanana, M., Rafahatelo, J.M., Randriamananjara, T., 2010. Geological evolution of the Antongil Craton. NE Madagascar. Precambrian Research 182, 187–203.
Shaw, R.K., Arima, M., Kagami, H., Fanning, C.M., Shiraishi, K., Motoyoshi, Y., 1997. Proterozoic events in the Eastern Ghats Granulite Belt, India: evidence from Rb–Sr, Sm–Nd systematics, and SHRIMP dating. Journal of Geology 105, 645–656.
Shiraishi, K., Hiroi, Y., Motoyoshi, Y., 1989. 1:250,000 Geological Map of Lützow-Holm Bay. National Institute of Polar Research, Tokyo, Japan.
Shiraishi, K., Ellis, D.J., Hiroi, Y., Fanning, C.M., Motoyoshi, Y., Nakai, Y., 1994. Cambrian orogenic belt in east Antarctica and Sri Lanka: implications for Gondwana assembly. Journal of Geology 102, 47–65.
Shiraishi, K., Hokada, T., Fanning, C.M., Misawa, K., Motoyoshi, Y., 2003. Timing of thermal events in eastern Dronning Maud Land, East Antarctica. Polar Geoscience 16, 76–99.
Shiraishi, K., Dunkley, D.J., Hokada, T., Fanning, C.M., Kagami, H., Hamamoto, T., 2008. Geochronological constraints on the Late Proterozoic to Cambrian crustal evolution of eastern Dronning Maud Land, East Antarctica: a synthesis of SHRIMP U-Pb age and Nd model age data. Geological Society, London, Special Publication 308, 21–67.
Song, B., Nutman, A.P., Dunyi, L., Jiashan, W., 1996. 3800 to 2500 Ma crustal evolution in the Anshan area of Liaoning Province, northeastern China. Precambrian Research 78, 79–94.
Stacey, J.S., Kramers, J.D., 1975. Approximation of terrestrial lead isotope evolution by a two-stage model. Earth and Planetary Science Letters 26, 207–221.
Takahashi, K., Tsunogae, T., Santosh, M., Takamura, Y., Tsutsumi, Y., 2017. Paleoproterozoic (ca. 1.8 Ga) arc magmatism in the Lützow-Holm Complex, East Antarctica: implications for crustal growth and terrane assembly in erstwhile Gondwana fragments. Journal of Asian Earth Sciences. http://dx.doi.org/10.1016/j.jseaes.2017.07.053 (submitted for publication).
Takamura, Y., Tsunogae, T., Santosh, M., Malaviarachchi, S.P.K., Tsutsumi, Y., 2015. Petrology and zircon U–Pb geochronology of metagabbro from the Highland Complex, Sri Lanka: implications for the correlation of Gondwana suture zones. Journal of Asian Earth Sciences 113, 826–841.
Takamura, Y., Tsunogae, T., Santosh, M., Malaviarachchi, S.P.K., Tsutsumi, Y., 2016. U–Pb geochronology of detrital zircon in metasediments from Sri Lanka: implications for the regional correlation of Gondwana fragments. Precambrian Research 281, 434–452.
Taylor, R.J.M., Clark, C., Fitzsimons, I.C., Santosh, M., Hand, M., Evans, N., McDonald, B., 2014. Post-peak, fluid-mediated modification of granulite facies zircon and monazite in the Trivandrum Block, southern India. Contributions to Mineralogy and Petrology 168, 1–17.
Taylor, R.J.M., Clark, C., Johnson, T.E., Santosh, M., Collins, A., 2015. Unravelling the complexities in high-grade rocks using multiple techniques: the Achankovil Zone of southern India. Contributions to Mineralogy and Petrology 169, 1–19.
Teale, W., Collins, A.S., Foden, J., Payne, J.L., Plavsa, D., Chetty, T.R.K., Santosh, M., Fanning, M., 2011. Cryogenian (830 Ma) mafic magmatism and metamorphism in the northern Madurai Block, southern India: a magmatic link between Sri Lanka and Madagascar? Journal of Asian Earth Sciences 42, 223–233.
Tsunogae, T., Dunkley, D.J., Horie, K., Endo, T., Miyamoto, T., Kato, M., 2014. Petrology and SHRIMP zircon geochronology of granulites from Vesleknausen, Lützow-Holm Complex, East Antarctica: Neoarchean magmatism and Neoproterozoic high-grade metamorphism. Geoscience Frontiers 5, 167–182.
Tsunogae, T., Yang, Q.Y., Santosh, M., 2015. Early Neoproterozoic arc magmatism in the Lützow-Holm Complex, East Antarctica: petrology, geochemistry, zircon U–Pb geochronology and Lu–Hf isotopes and tectonic implications. Precambrian Research 266, 467–489.
Tsunogae, T., Yang, Q.Y., Santosh, M., 2016. Neoarchean–Early Paleoproterozoic and Early Neoproterozoic arc magmatism in the Lützow–Holm complex, East Antarctica: insights from petrology, geochemistry, zircon U–Pb geochronology and Lu–Hf isotopes. Lithos 263, 239–256.
Tsutsumi, Y., Miyashita, A., Terada, K., Hidaka, H., 2009. SHRIMP U–Pb dating of detrital zircons from the Sanbagawa Belt, Kanto Mountains, Japan: need to revise the framework of the belt. Journal of Mineralogical and Petrological Sciences 104, 12–24.
Tsutsumi, Y., Horie, K., Sano, T., Miyawaki, R., Momma, K., Matsubara, S., Shigeoka, M., Yokoyama, K., 2012. LA-ICP-MS and SHRIMP ages of zircons in chevkinite and monazite tuffs from the Boso Peninsula, Central Japan. Bulletin

of the Natural Museum of Nature and Science, Series C (Geology and Paleontology) 38, 15–32.
Tucker, R.D., Roig, J.Y., Macey, P.H., Delor, C., Amelin, Y., Armstrong, R.A., Rabarimanana, M.H., Ralison, A.V., 2011. A new geological framework for south-central Madagascar, and its relevance to the "out-of-Africa" hypothesis. Precambrian Research 185, 109–130.
Willbold, M., Hegner, E., Kleinschrodt, R., Stosch, H.-G., Kehelpannala, K.V.W., Dulski, P., 2004. Geochemical evidence for a Neoproterozoic magmatic continental margin in Sri Lanka-relevance for the Rodinia-Gondwana supercontinental cycle. Precambrian Research 130, 185–198.
Williams, I.S., 1998. U–Th–Pb geochronology by ion microprobe. In: McKibben, M.A., Shanks, W.C. (Eds.), Applications of microanalytical techniques to understanding mineralizing processes. Reviews in Economic Geology 7, 1–35.
Yoshida, M., Funaki, M., Vitanage, P.W., 1992. Proterozoic to Mesozoic East Gondwana: the juxtaposition of India, Sri Lanka, and Antarctica. Tectonics 11, 381–391.
Yoshimura, Y., Motoyoshi, Y., Miyamoto, T., Grew, E.S., Carson, C.J., Dunkley, D.J., 2008. High-grade metamorphic rocks from Skallevikshalsen in the Lützow-Holm Complex, East Antarctica: metamorphic conditions and possibility of partial melting. Polar Geoscience 17, 57–87.